PREDICTION OF UNDRAINED SHEAR STRENGTH AND SWELLING PRESSURE OF FINE GRAINED SOIL USING ARTIFICIAL NEURAL NETWORK BASED MODEL: THE CASE OF KOYE FECHE SITE

MSc. THESIS

BY TEFERI WORKAFERAHU

HAWASSA UNIVERSITY, HAWASSA, ETHIOPIA

DECEMBER 2020

PERDICTION OF UNDRAINED SHEAR STERNGTH AND SWELLING PRESSURE OF FINE GRAINED SOIL USING ARTIFICIAL NEURAL NETWORK BASED MODEL: THE CASE OF KOYE FECHE SITE

TEFERI WOKAFERAHU

THESIS SUBMITTED TO THE
DEPARTMENT OF CIVIL ENGINEERING, FACULTY OF CIVIL AND BUILT ENVIRONMENT, HAWASSA UNIVERSITY INSTITUTE OF TECHNOLOGY, SCHOOL OF
GRADUATE STUDIES, HAWASSA UNIVERSITY

IN PARTIAL FULFILLMENT OF THE REQUIREMENTS FOR THE
DEGREE OF
MASTER OF SCINCE IN GEOTECHNICAL ENGINEERING

DEC 2020

SCHOOL OF GRADUATE STUDIES

HAWASSA UNIVERSITY

ADVISORS' APPROVAL SHEET

This is to certify that the thesis entitled "PREDICTION OF UNDRAINED SHEAR STRENGTH AND SWELLING PRESSURE USING ARTIFICIAL NEURAL NETWORK BASED MODEL: THE CASE OF KOYE FICHE SITE" and submitted in partial fulfillment of the requirements for the degree of Master's with specialization in GEOTECHNICAL ENGINEERING, the Graduate Program of the School of Civil Engineering, and has been carried out by TEFERI WORKAFERAHU SEMUNIGUS ID. No PGGeo/036/09, under my supervision. Therefore, we recommend that the student has fulfilled the requirements and hence hereby can submit the thesis to the department.

Mr. M U Jagadeesha	----------	----------
Major Advisor	signature	Date

SCHOOL OF GRADUATE STUDIES

HAWASSA UNIVERSITY

EXAMINERS' APPROVAL SHEET

We, the undersigned, members of the Board of Examiners of the final open defense by **TEFERI WORKAFERAHU SEMUNIGUS** have read and evaluated his Thesis entitled "PREDICTION OF UNDRAINED SHEAR STRENGTH AND SWELLING PRESSURE USING ARTIFICIAL NEURAL NETWORK BASED MODEL: THE CASE OF KOYE FICHE SITE", and examined the candidate. This is, therefore, to certify that the thesis has been accepted in the partial fulfillments of the requirements for the degree of Master with specialization in Geotechnical Engineering.

Mr. Desta A.	…….	……..
Chairperson	Signature	Date
Mr. M U Jagadeesha (PhD)	…….	……..
Major Advisor	Signature	Date
Mihret Dananto (PhD)	…….	……..
Internal Examiner	Signature	Date
Tensay Gebremedhin (PhD)	…….	……..
External Examiner	Signature	Date
……..	…….	……..
SGS Approval	Signature	Date

DEDICATION

I dedicate this thesis to my uncle (Abraham) he scarifies for my success and support me at any situation.

DECLARATION

I, Teferi Workaferahu, declare that this MSc. Thesis is my own original work and has not been presented for a degree in any other university, and all sources of materials used for this thesis have been duly acknowledged.

Name ---------- Signature ----------

Date of submission ----------

ACKNOWLEDGEMENTS

Above all, I would like to thank almighty God without His support and blessing, it could not have been possible all my wishes to come in to the reality.

I would like to express my deepest gratitude to Mr. M U Jagadeesha for his close supervision, valuable, constructive & timely guidance at all the stages of the study.

Finally, my appreciation and thanks goes to my family who gave me all the energy and friends relatives who have helped me in any form of support which are greatly needed for the advancement and completion of this work.

Table of Content

LIST OF TABLES

LIST OF FIGURES

LISTS OF ACRONYMS AND ABBREVATIONS

AI	Artificial Intelligence
ANN	Artificial neural network
C	Clay particle
Cu	Undrained shear strength
CEC	Cation exchange capacity
IEEE	Institute of Electrical and Electronic Engineer's
logsig	Logarithmic sigmoidal transferfunction
LL	Liquid limit
MRA	Multiple regression analysis
MLP	Multi-layer perceptions
N	Number of neuron
PI	Plasticity index
Ps	Swelling pressure
Purlin	Pure linear
q_u	Unconfined compressive strength
RMSE	Root mean squared error
R	Correlation coefficient
tansig	Tangent sigmoidal
W	Water content
W_I	Initial water content

Wn	Natural water content
LLm	Modified liquid limit
PIm	Modified plastic index
ρ_d	Dry unit weight

ABSTRACT

This research presents an Artificial Neural Network based correlation of undrained shear strength and swelling pressure with the standard index test results of Koye-Feche fine grained soil. Simple index test results used for the analysis include unit weight, natural moisture content, liquid limit, plastic limit, liquidity index and plasticity index. Unlike conventional methods, ANNs do not depend on simplified assumptions, have universal function approximation capacity, noisy or missing data resistance, accommodate multiple nonlinear variables for unknown interactions, and have a good generalization capability. A total of four models were proposed for prediction. The first three models were produced for Cu while the remaining one was developed for Ps. Swelling pressure and undrained shear strength were trained in an ANNs program and the results were compared with the experimental values. An automated optimization script has also been developed that can be successfully used to pick the optimal network architecture. Performance indices (i.e. Correlation coefficient and root mean square error) were computed to check the prediction capacity of the ANN models. The devised ANN model was compared with the conventional regression analysis and found superior in all cases. The results obtained from ANN and existing empirical formulas were compared to those obtained from the experiments. It was found that the values predicted from the ANN models match the experimental values much better than those obtained from the equations. Undrained shear strength results showed a strong correlation with the combined Liquid Limit and Plasticity Index input parameters. Whereas, Dry unit weight, natural moisture content, liquid limit and plastic index are powerful predictor of swelling pressure. It has been verified that the ANN models can be used satisfactorily to predict undrained shear strength and swelling pressure as a rapid inexpensive substitute for laboratory techniques. Further research should be conducted to extend all aspects of this research, such as by collecting more data in order to improve results.

Keyword: Artificial neural network, Swelling pressure, Undrained shear strength, Index property

1. INTRODUCTION

1.1. Background

Every structure resting on the surface and sub-surface of the ground requires safe and stable soil base. Safety and stability fulfillment requires careful investigation of engineering properties of the soil. However, obtaining these engineering properties of soils needs relatively more time and money. There are several methods developed for the determination of soil properties, so far. Laboratory tests like triaxial compression test and oedometer test are conducted to determine q_u and Swelling Pressure, respectively. The determination of realistic values from these tests requires special techniques such as, the preparation of undisturbed soil sample and the consideration of initial overburden pressure.

When the extent of construction is very large correlations are important of any project to predict geotechnical parameters from simple and available test results. Relations developed between index properties and laboratory test results in fine-grained soil predict undrained shear strength and swelling pressure with ease. The prediction of these properties can also be performed using Artificial Neural Network based approach.

Artificial intelligence (AI) has been shown high predictive ability comparing to traditional methods and because of that, it became widely usable in modeling the complex behavior of most geotechnical engineering materials. Starting from 90s, there is increasingly in employed AI as an effective tool in geotechnical engineering. AI techniques are artificial neural networks (ANNs), genetic programming (GP), evolutionary polynomial regression (EPR), support vector machines, M5 model trees, and K-nearest neighbors (Elshorbagyet.al 2010).

The idea of artificial neural network technology is similar to the brain's own problem-solving process and successfully applied in geotechnical engineering (Elshorbagyet.al. 2010).

ANN is an adaptive system that changes its structure based on external or internal information that flows through the network during the learning phase (Farrokhzad, et.al, 2010).

An ANN processes information using simple interconnected elements known as neurons, which are located in distinct layers of the network. The best type of ANN, the multi-layer perceptron (MLP), consists of at least three layers: an input layer, an output layer, and intermediate or

hidden layer(s) (Meulenkamp and Grima, 1999). Each layer comprises one or more nodes (neurons). The lines between the nodes indicate the flow of information from one node to the next ((Edy Tonnizam and Danial Johad, 2014).

An artificial neural network (ANN), usually called neural network (NN), is a mathematical model or computational model that is inspired by the structure and/or functional aspects of biological neural networks (Haryana, 2017).

Artificial Neural Networks are relatively crude electronic models based on the neural structure of the brain. The brain basically learns from experience. It is natural proof that some problems that are beyond the scope of current computers are indeed solvable by small energy efficient packages. This brain modeling also promises a less technical way to develop machine solutions. This new approach to computing also provides a more graceful degradation during system overload than its more traditional counterparts (Dave Anderson and George McNeill, 1992).

The Brain would be considered a Natural Neural Network, comprised of hundreds of billions of neurons, each interconnected with thousands of others. Scientists believe that this interconnection between neurons is what enables us to think, reason, and rationalize solutions to problems that cannot be solved analytically. No one knows how brains actually function and how humans have the ability to reason and learn, but one can only design models that are vaguely similar (Wasserman, 1989).

The Standard Penetration Test (SPT) is one of the most commonly used in-situ tests for site investigation and foundation design. SPT is a common field test to predict the behavior of coarse-grained soils. However, it used widely in all types of soil due to its simplicity and cost effectiveness (Singh et.al, 2017). Many empirical correlations have been developed between the SPT N-value, and other engineering properties of the soil including q_u. SPT is mainly useful under conditions of financial and time limitations in a project as also where obtaining undisturbed samples of soil becomes difficult (Jibahand,2017).

SPT capability to estimate undrained shear strength of fine-grained soil the parameters of natural water content (wn), liquid limit (LL) and plasticity index (PI) considered as independent effective parameters, in addition to N (SPT) (Nassaji, et.al. 2011).

The investigation of index properties for a soil is much easier than investigating other engineering properties; in terms of time, money, effort and quality. Moreover, most engineering properties of soils depend up on their index properties. Therefore, by obtaining the index property of soils that involves simpler and quicker method of testing, the engineering properties can be predicted satisfactorily from empirical correlations.

To develop NN architecture of swelling pressure liquid limit, plastic index, natural moisture content and dry unit weight combination have very good prediction capability and for undrained shear strength prediction SPT-N, liquid limit and plastic limit are reliable.

1.2. Statement of the Problem

Oedometer and Unconfined compressive strength tests are time-consuming compared to standard index tests. Various attempts have been made to estimate undrained shear strength and swelling pressure from simple tests that can be carried out more easily. Empirical formulas relating various parameters with undrained shear strength and swelling pressure have been presented by many researchers. In estimating the swelling pressure and undrained shear strength, most researchers have used single or dual-parameter models, such as the liquid limit, natural water content, dry unit weight, and others. The main criticism of these techniques is that the complex mechanism of the swelling and strength characteristic is oversimplified, and the different parameters of the soil are not adequately taken into account. When multiple variables are considered to increase the predictability of the empiric formula, the variables used in the regression formula are likely to be correlated, leading to complex multicollinearity problems. A formula capable of resolving the complexities between the dependent variable and the associated soil parameters is therefore required.

Unlike ANN approaches, most traditional empirical and statistical methods, require prior knowledge about the nature of the relationships among the data. Moreover, ANNs can handle imperfect or incomplete data and can capture non-linear and complex relationships between system variables. Conventional methods have the following drawbacks:

- Depend on simplified assumptions such as linear behavior
- Less resistance to noisy or missing data
- Accommodation of linear variables for unknown interactions

However, there is no need to make assumptions when using ANNs on what could be the underlying rules that govern the problem in hand. In addition, ANNs are advantageous in such a way that the system possesses universal function approximation capacity, resistance to noise or missing data, accommodation of multiple nonlinear variables for unknown interactions and good generalization capability.

Overall, a number of studies on correlation studies have been performed on a local basis. However, these studies are based solely on conventional methods. Thus, this paper describes the implementation of an artificial neural network (ANN) using a few variables to address the limitation of empirical formulas obtained from regression analysis.

1.3. Research Questions

- How does artificial neural network and conventional or empirical methods compare in terms of producing better prediction performance?
- What input parameters have better predictive performance of undrained shear strength?
- What input parameters have better predictive performance of swelling pressure?

1.4. Objective of the Study

1.4.1. General Objective

The general objective of this study is to predict swelling pressure and undrained shear strength of some fine-grained soils found in Koye-Feche by using artificial neural network based model.

1.4.2. Specific Objective

- To develop an artificial neural network model for prediction of undrained shear strength and swelling pressure.
- To compare the developed model with the conventional regression analysis prediction method.
- To compare the developed model with previously developed empirical equations.

1.5. Scope of the Study

This research covers the prediction of swelling pressure and undrained shear strength of some fine-grained soil found in Koye-Feche area by using ANN. The test data was collected from actual site investigation reports. Thus, the data was gathered from governmental organization of Addis Ababa housing construction office.

After the completion of the prediction the performance of ANNs model will be assessed and attempted to evaluate whether previously developed models for soil in other area by other researchers can predict the swelling pressure and unconfined compressive strength of the soil in the selected study area or not.

The research focuses on presenting an alternative way of computing some properties like swelling pressure and undrained shear strength by using ANN based training algorithm.

1.6. Significance of the Research

Constraints like financial limitation, unavailability of equipment and time limitation made the correlation between engineering properties of soil inevitable. Therefore, the development of efficient prediction model is crucial. When the extent of construction is very large, a lot of swelling pressure, undrained shear strength and index property tests have to be performed. Obtaining the properties of fine-grained soil requires relatively detail laboratory procedures and it is time consuming. Thus, it is crucial to obtain the index property parameters that involve relatively simpler, quicker, and cheaper method of testing to predict strength characteristics satisfactorily by using ANNs than conventional methods, if optimized properly. An important advantage of using Artificial Neural Network (ANN) over regression in process modeling is its capacity in dealing with multiple outputs or responses while each regression model is able to deal with only one response.

2. LITERATURE REVIEW

2.1. General

In many cases various types of relationships may be needed to estimate the geotechnical parameters from the values that are extracted from the in-situ tests. One of these important parameters is undrained shear strength known with Cu (or Su). Cu could be estimated from the in-situ tests such as pocket penetrometer, cone penetration test (CPT), standard penetration test (SPT) and vane shear test (VST). SPT is one of the simplest, cheapest and most widely used tests that are used in many geotechnical projects in worldwide (Nassaji & Kalantari, 2011).

SPT capability to estimate undrained shear strength of fine-grained soil in the southern as well as eastern of Tehran (Iran) using the multi linear regression analysis from SPSS software was investigated in two phases. In the first phase, only N (SPT) considered as independent parameter, but in the second phase the parameters of natural water content (wn), liquid limit (LL) and plasticity index (PI) considered as independent effective parameters, in addition to N (SPT). The regression analysis of data revealed that relationships in the second phase have better correlation than first phase (Nassaji & Kalantari, 2011).

The feasibility and efficiency of applying artificial neural networks (ANN) to predict ϕ (angle of internal friction), E (modulus of elasticity) and qc (CPT result) from SPT results (N values) and concluded that it shows a very good agreement with actual results compared to some of the traditional methods available in the literature (Hafez et.al, 2017).

Expansive soils exhibit significantly high volumetric deformations and pose a serious threat to stability of the structures and foundations. Thus, determination of their swelling properties (i.e. swelling potential and swelling pressure) becomes essential. However, measurement of the swelling properties is time-consuming and requires special and expensive equipment (Erzin & Gunes, 2011). A comparison between multiple regression analysis (MRA) model and ANN model for predicting swelling pressure of clay. They used the swelling pressures of six types of soils from northern part of Jordan using the free swell test, the constant volume swell test and the swell overburden test. The results showed that ANN was very efficient in predicting clay swelling pressure and was superior to MRA (Barakat & Attom, 1999).

2.2. History of Artificial Neural Networking

The study of the human brain is thousands of years old. With the advent of modern electronics, it was only natural to try to harness this thinking process. The first step toward artificial neural networks came in 1943 when Warren McCulloch and Walter Pitts, wrote a paper on how neurons might work. They modeled a simple neural network with electrical circuits. Reinforcing this concept of neurons and how they work was a book written by Donald Hebb. The Organization of Behavior was written in 1949. It pointed out that neural pathways are strengthened each time that they are used. As computers advanced into their infancy of the 1950s, it became possible to begin to model the rudiments of these theories concerning human thought. Yet, throughout this time, advocates of "thinking machines" continued to argue their cases. In 1956 the Dartmouth Summer Research Project on Artificial Intelligence provided a boost to both artificial intelligence and neural networks. In the years following the Dartmouth Project, John von Neumann suggested imitating simple neuron functions by using vacuum tubes (Dave A. and George Mc., 1992).

In 1982, Hopfield's approach was not to simply model brains but to create useful devices. With clarity and mathematical analysis, he showed how such networks could work and what they could do. He was articulate, likeable, and a champion of a dormant technology. At the same time, another event occurred. A conference was held in Kyoto, Japan. This conference was the US-Japan Joint Conference on Cooperative/Competitive Neural Networks. Japan subsequently announced their Fifth Generation effort. By 1985 the American Institute of Physics began what has become an annual meeting Neural Networks for Computing. In 1987, IEEE first International Conference on Neural Networks made. By 1989 at the Neural Networks for Defense, meeting Bernard Windrow told his audience that they were engaged in World War IV, "World War III never happened," where the battlefields are world trade and manufacturing. (Dave A. and George McNeill, 1992).

Today, neural networks discussions are occurring everywhere. Their promise seems very bright, as nature itself is the proof that this kind of thing works. Yet, its future, indeed the very key to the whole technology, lies in hardware development (Dave A. and George McNeill, 1992).

2.3. Properties of Fine Grained Soil

Soils are often separated into coarse-grained soils and fine-grained soils. Coarse-grained soils include boulders, cobbles, gravel and sand, whereas fine-grained soils consist of clays and silts (Fratta et.al, 2007). The engineering properties of fine-grained soils are strongly dependent on water content. They are susceptible to changes in external pressure, chemistry of the pore medium, wetting and drying cycles and temperature (Sridharan, 1990).

Probably the most important grain property of fine-grained soils is the mineralogical composition. The complexity in the engineering behavior of fine-grained soils is attributable mostly to the clay size fraction of the soil. Most soil classification systems arbitrarily define clay particles as having an effective diameter of 2μmor less and do not account for the clay mineral type. Furthermore, the influence of the force of gravity on each particle is insignificant compared with that of the electrical forces acting at the surface of the particle (Terzaghi et.al, 1996; Sridharan, 1990).

The properties of fine-grained soils may vary considerably between their natural condition in the ground and their state after being disturbed, even if moisture content does not change. Fine-grained clay-rich soils can absorb large quantities of water after rainfall, becoming sticky and heavy. Conversely, they can also become very hard when dry, resulting in shrinking and cracking of the ground (Mitchell, 1976).

Fine-grained soils have poor load-bearing capacities compared with coarse-grained soils. Fine-grained soils are practically impermeable, change volume and strength with variations in moisture conditions, and are susceptible to frost. Mineralogical factors rather than grain size control the engineering properties of fine-grained soils. Thin layers of fine-grained soils, even within thick deposits of coarse-grained soils, have been responsible for many geotechnical failures, and therefore, you need to pay special attention to fine-grained soils (Budhu, 2015).

If the soil is a fine-grained soil (clay), the construction period is short compared to the time required to dissipate the excess pore pressure induced by the load. Undrained conditions simulate this load process (Nova, 2010).

2.4. Undrained Shear Strength

Undrained shear strength is one of the useful parameters in order to take engineering decisions. Most often, the bearing capacity is estimated based on undrained shear strength to make conservative estimates. Some laboratory tests needed to obtain these values are expensive and time consuming, while soil properties like moisture content and Atterberg limits can be performed faster and cheaper. Many empirical formulae are available to estimate the Cu for fine-grained soils like clay or silt (Muduruet.al, 2014).

The q_u test is a special case of a triaxial compression test in which the all-round pressure($\sigma_3 = 0$). The test is applicable only to fine grained soils such as saturated and unsaturated clays that have shear strength without confining pressure (Fratta et.al., 2007). The test is an undrained test and is based on the assumption that there is no moisture loss during the test.

The unconfined compressive strength is considered to be equal to the load at which failure occurs, or at which the axial strain reaches 20% if there is no sudden failure, divided by the cross-sectional area of the sample at the time of failure (Terzaghi et.al, 1996).

When a soil specimen fails, one half the stress at that point is referred to as the undrained shear strength (Fratta et.al, 2007).

Laboratory test results can be interpreted as follows,

$$\text{axial strain, } \varepsilon_a = \left(\frac{\Delta H}{H_o}\right) * 100 \qquad \text{stress, } \sigma = \frac{F}{A_c}, \text{ where, } A_c = \frac{A_i}{1-\varepsilon} \tag{1}$$

Where load (in kg-force) and strain in (mm) and A_i is the initial area of the specimen (πr_i^2)

According to (Hara et.al, 1974) undrained shear strength (c_u) is given by, $c_u = 0.5 * q_u$
Where, q_u is unconfined compressive strength.

Table 2.1 Consistency and unconfined compressive strength of clays

Consistency	$q_u\ (kN/m^2)$
Very soft	0-24
Soft	24-48
Medium	48-96
Stiff	96-192
Very stiff	192-383
Hard	>383

2.5. Swelling Pressure

2.5.1. General

The swelling of soils, in general, is due to the presence of expansive clay minerals, hydration of cations on clay surfaces, and release of intrinsic stresses caused by over consolidation or desiccation of soils. (Dhowian et.al, 1998) Swelling pressure is a very useful index of the trouble potential of an expansive soil. This pressure is the maximum force per unit area that needs to be applied over a swelling soil to prevent volume increase.

Swelling Pressure is the amount of pressure a soil exerts upon swelling or the pressure required recompressing the fully swollen sample back to its initial volume. Most of the structural damages occur when the swelling pressure is greater than the foundation pressure, assessing the swelling pressure is an important task in dealing with expansive soil (Alemayehu Teferra & Mesfin, 1999).

Expansive soils are that clay soils which exhibit significant volume changes because of soil moisture variation. Expansive soils are a worldwide problem that poses several challenges to civil engineers. Foundations constructed on these clays are subjected to large uplift forces caused by swelling, and inducing heaving, cracking, and break up of both building foundations and slabs on grade members. Heave problems account for more economic loss than all other soil problems. (Dhowian et.al, 1998).

Expansive soil is known to be widely spread in Ethiopia. Although the extent and range of distribution of this problematic soil has not been studied thoroughly: the southern, south-east

and south-west part of the city of Addis Ababa areas, where most of the recent construction are being carried out and central part of Ethiopia following the major trunk roads like Addis-Ambo, Addis-Woliso, Addis-Debre Birhan, Addis-Gohatsion, Addis-Modjo. In addition, areas like Bahir Dar, Mekele, and Gambela etc. are partly covered by Expansive soil (Zewdie, 2004).

Expansive soil has caused a number of problems in most structures constructed in Addis Ababa. Recent researches in assessing the failures caused on structures built on expansive soils showed that more than 60% of the structures are damaged due to causes associated with expansive soils (Seed et.al, 1962).

2.5.2. Measurement of Swelling Pressure

Swelling pressure can be determined by direct or indirect methods. Available techniques for quantitative measurement swelling pressure of expansive soils can be categorized into three groups. Namely, oedometer tests, soil suction tests and empirical methodology (Alemayehu Teferra & Mesfin, 1999). There are several indirect measurement methods used to predict swell potential of expansive soil s and these methods are summarized below (Douglas & George, 2003).

2.5.2.1. Index property

Soils occur naturally in a large variety. Engineers are continually searching for simplified tests that will increase their knowledge of soils by employing a simple and rapid soil tests. These simplified tests that are indicative of the engineering properties of soils are called index properties. Index properties of cohesive soils are used to characterize the physical and mechanical behavior of soils by making use of parameters such as Moisture Content, Dry Density, Specific Gravity, particle size distribution, and Atterberg Limits. Such parameters are useful to provide correlations with engineering soil properties for the estimation of swelling potential of expansive soils.

The Atterberg consistency limits of soils are used for the purpose of classification of cohesive soil materials for engineering purposes. The Atterberg limits are widely related to the shear strength, bearing capacity, compressibility, swelling potential and specific surface of soils. The plastic limits assume a lot of importance to obtain information on soil mechanical behavior (Muduru Srimurall and K.Nagenders Prasad, 2014).

2.5.2.2. Modified liquid limit and modified plasticity index

The Atterberg limits are usually conducted for soil fraction passing 425 microns. The values thus obtained may not be true representation of the entire soil. The presence of coarse particles only dilutes the physcio-chemical potential of the soil proportionately (Muthy V.N.S. 1987). Accordingly, the modified liquid limit (LLm) and modified plasticity index (PIm) are defined to analyze the test results.

$$\text{Modified liquid limit (LLm)} = LL \times F/100 \quad (2)$$

$$\text{Modified plasticity index (PIm)} = PL \times F/100 \quad (3)$$

Where, F is fraction passing through 425 microns

2.6. Artificial Neural Network

2.6.1. Introduction

Artificial neural networks (ANNs) are a form of artificial intelligence, which attempt to mimic the function of the human brain and nervous system. ANNs learn from data examples presented to them in order to capture the understated functional relationships among the data even if the underlying relationships are unknown or the physical meaning is difficult to explain. This is in contrast to most traditional empirical and statistical methods, which need prior knowledge about the nature of the relationships among the data. ANNs are thus well suited to modeling the complex behavior of most geotechnical engineering materials, which, by their very nature, exhibit extreme variability. This modeling capability, as well as the ability to learn from experience, have given ANNs superiority over most traditional modeling methods since there is no need for making assumptions about what the underlying rules that govern the problem in hand could be. (M. A. Shahin & Maier, 2008)

Although developing an analytical or empirical model is feasible in some simplified situations, most manufacturing processes are complex, and therefore, models that are less general, more practical, and less expensive than the analytical models are of interest. An important advantage of using Artificial Neural Network (ANN) over regression in process modeling is its capacity in dealing with multiple outputs or responses while each regression model is able to deal with only one response. Another major advantage for developing NN process models is that they do

not depend on simplified assumptions such as linear behavior or production heuristics. Neural networks possess a number of attractive properties for modeling a complex mechanical behavior or a system: universal function approximation capability, resistance to noisy or missing data, accommodation of multiple nonlinear variables for unknown interactions, and good generalization capability (Park, 2011).

2.6.2. The Concept of Artificial Neuron

Much is still unknown about how the brain trains itself to process information, so theories abound. In the human brain, a typical neuron collects signals from others through a host of fine structures called dendrites (Figure 2.1). The neuron sends out spikes of electrical activity through a long, thin stand known as an axon, which splits into thousands of branches. At the end of each branch, a structure called a synapse converts the activity from the axon into electrical effects that inhibit or excite activity from the axon into electrical effects that inhibit or excite activity in the connected neurons. When a neuron receives excitatory input that is sufficiently large compared with its inhibitory input, it sends a spike of electrical activity down its axon. Learning occurs by changing the effectiveness of the synapses so that the influence of one neuron on another changes. An artificial neuron is a device with many inputs and one output. The neuron has two modes of operation; the training mode and the using mode. In the training mode, the neuron can be trained to fire (or not), for particular input patterns. In the using mode, when a taught input pattern is detected at the input, its associated output becomes the current output. If the input pattern does not belong in the taught list of input patterns, the firing rule is used to determine whether to fire or not (Dave Anderson and George McNeill, 1992).

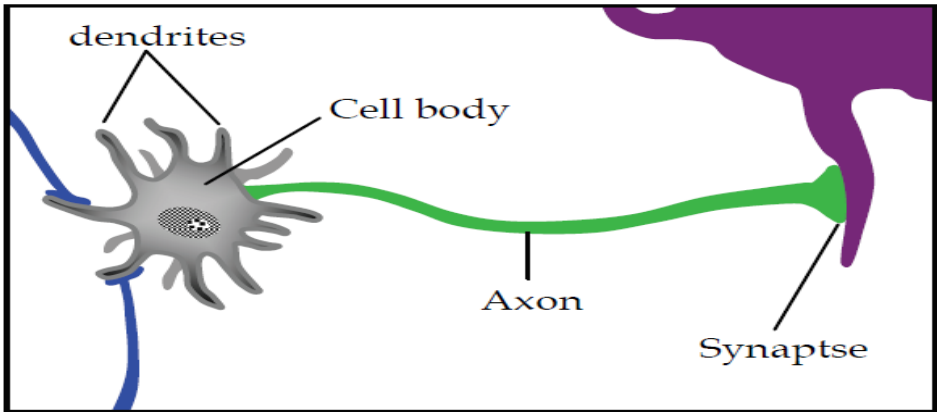

Figure 2.1 Biological Neuron

The fundamental processing element of a neural network is a neuron. This building block of human awareness encompasses a few general capabilities. A biological neuron receives inputs from other sources, combines them in some way, performs a generally nonlinear operation on the result, and then outputs the final result (Anderson & McNeill, 1992).

2.6.3. How Artificial Neural Networks Work

The ANN uses a set of examples in a training database as input, a learning algorithm to adjust the weights and an activation function to derive an output. If the connection weight between the neurons is changed, the relationship of the network's output to its input will be altered. The process of adjusting the connection weights by repeatedly exposing the network to known input-output data is called training. The error back-propagation learning method is popular and successful training technique. A trained ANN can take inputs and produce outputs very quickly, which is an advantage in doing optimization in the proposed approach (Agrawal et.al, 1997).

The architecture of a supervised ANN, generally, consists of an input layer, an output layer and one or more hidden layers. The input layer contains the input variables. The output layer contains the target output vector. At least one hidden layer that contains the artificial neurons (processing units) is used between the input and output to assist in the learning process. The neurons in the different layers are interconnected. Each connection has a 'weight' associated with it. Input values in the first layer are weighted and passed on to the hidden layer. Neurons in the hidden layer produce outputs by applying an activation function to the sum of the weighted input values (Goh, 1995a; Specht, 1991).

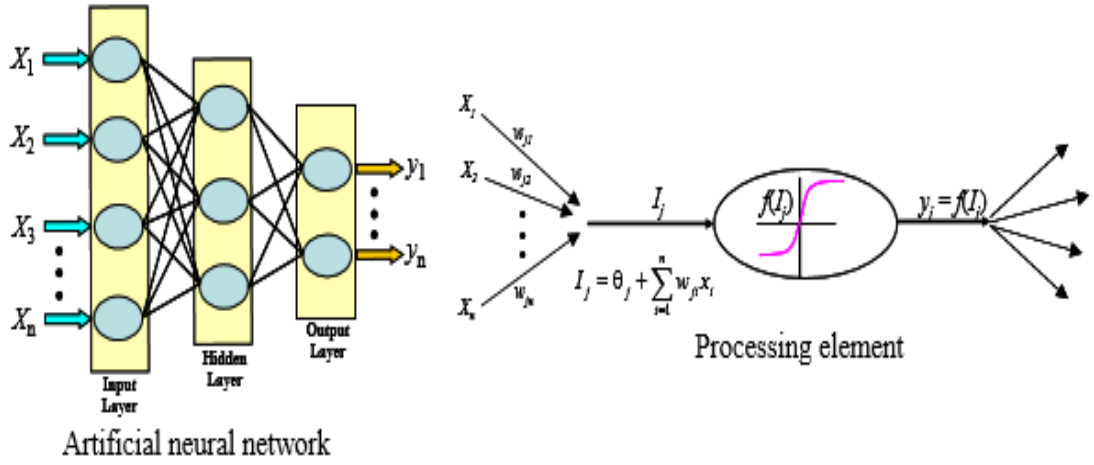

Figure 2.2 Typical structure and operation of ANNs

where, I_j = the activation level of node j

w_{ji} = the connection weight between nodes j and i

x_i = the input from node i, i = 0,1 …

θ_j = the bias or treshold for node j

y_i = the output of node j and

$f(.)$ = the transfer function

2.7. Previous Studies

2.7.1. Prediction of Undrained Shear Strength

Terzaghi& Peck, (1967), were the first to predict undrained shear strength from q_u – SPT (N) values of fine-grained soils. Sanglerat, (1972) studied fine-grained soils and presented the correlation by considering plasticity index of clay soil and thus he divided the soils into clay and silty clay (Stroud, 1974) proposed one of the most popular relationships between SPT- N values and Cu. In his study, SPT- N data were collected from many sites in the United Kingdom together with triaxial tests performed in insensitive stiff and hard clays. He observed that Cu decrease with increasing PI in a constant N value for PI< 30 %. However, the results of Sowers

(1979) shows that Cu increases with increasing in plasticity index. Other researchers who tried to determine the correlation between q_u – SPT (N) are summarized in the table below.

Table 2.2 Previous correlations of UCS

Researcher	Explanation	UCS(kPa)
Sanglerat, 1972	Clay and silty clay	12.5N, 10N
Terzaghi& Peck, 1967	Fine-grained soil	6.25N
Hara et al., 1974	Fine-grained soil	$29N^{0.72}$
Sowers, 1979	Highly, medium and low plastic soil	12.5N, 7.5N, 3.75N
Nixon, 1982	Clay	12N
Stroud, 1974	PI<20, 20<PI<30, PI>30	(6-7)N, (4-5)N, 4.2N
Decourt, 1990	Clay	12.5N and 15N60
Ajayi & Balogun, 1988	Fine-grained soil	1.39N+74.2
Hettiarachchi& Brown, 2009	Fine-grained soil	4.1N60
Sirvikaya, 2009	UCS test	$2.41N–0.82w_n + 0.14LL + 1.44PI$
Wroth & Wood, 1978	Clay	$170e^{-4.6LI}$

Where w_n-natural moisture content, N-standard penetration test (number of blows), LL-liquid limit, PI-plasticity index, LI-liquidity index, Cu-undrained shear strength

2.7.2. Prediction of Swelling Pressure

Many relationships have been developed to estimate swelling pressure from index test and the physical state of the soil. Some of them proposed by different researchers are listed below.

Table 2.3 Previous correlation of swelling pressure

Researcher	Ps (swelling pressure)
Komornik& David, 1969	$\log Ps = 0.132 * LL + 0.0006688 * \gamma_d - 0.0269 * w$
Vijayavergiya & Ghazzaly, 1973	$\log Ps = \frac{1}{12}(0.4 * LL - w + 23.6)$
Nayak& Christensen, 1974	$\text{Ps} = 2.5 * 10^{-1}(PI)^{1.12} * \frac{c^2}{w_i^2} + 25$
Teklu, 2003	$\log Ps = -5.00 - 0.0002064 * LL + 0.003477 * PI + 0.005827 * \gamma_d$
Ashenafi T., 2013	$Ps = 1.639 * \gamma_d + 32.676 * PL - 3110.94$
Abdishkur K., 2015	$Ps = 965.22 + 38.53 * \frac{\gamma_d}{\gamma_\cdot} - 26.99 * w + 8.68 * PL - 3110.94$
Asamnew G., 2016	$Ps = 1.5197 * \gamma_d + 0.3042 * PI - 31.4295$

Where, Ps-swelling pressure, $\frac{\gamma_d}{\gamma_\cdot}$ – dry density/effective density, C-clay content, w_i–initial water content, w-water content, γ_d- dry unit weight

2.7.3. Prediction using ANN Model in Geotechnical Engineering

The swelling potentials of soils to develop a statistical model and ANN models. Both ANN models were found to be able to predict swelling potential more accurately than the statistical model. (Barakat and Attom, 1999) presented a comparison between multiple regression analysis (MRA) model and ANN model for predicting swelling pressure of clay. They used the swelling pressures of six types of soils from northern part of Jordan using the free swell test, the constant

volume swell test and the swell overburden test. The results showed that ANN was very efficient in predicting clay-swelling pressure and was superior to MRA.

Erzin (2008) and Erzin and Gunes (2011) attempted to predict the swell pressures of clayey soils by using ANNs. He used, the constant volume swells tests in oedometers (ASTM 1990) (Erzin, 1997; Erzin & Erol, 2004) performed on statically compacted specimens of Bentonite-Kaolinite clay mixtures with varying soil properties were used. The ANNs results were compared with experimental ones and found close to them. Moreover, the values of the variance (VAF) and the root mean square error (RMSE) indices were calculated to check the prediction performance of the ANN models developed. ANN model has shown high prediction performance according to the performance indices.

Based on the application of ANNs, methodologies have been developed for estimating several soil properties

- Pre-consolidation pressure (Celik and Tan, 2005)
- Shear strength and stress history (Kurup and Dudani 2002; Lee et al. 2003; (Penumaduet al., 1994; Yang and Rosenbaum, 2002)
- Swell pressure (Naijar, Basheer, & McReynolds, 1996; Erzin Y., 2007)
- Compaction and permeability (Agrawal et al., 1994; Goh 1995b; Gribb, 1994; Naijar, et.al, 1996b; Sinha and Wang, 2008) and
- Soil classification (Cal, 1995)

3. MATERIALS AND METHODS

3.1. Description of the Study Area

3.1.1. Location

The study area is located Addis Ababa, Akaki Kaliti sub-city around Koye Feche Locality. The site is characterized by flat to rolling ground with an average elevation of 2200m a.s.l. Associations house and Addis-Adama express highway, that extend from Tulu Dimtu to CMC exist. Addis Ababa housing construction office constructed condominium houses in this area. Koye Feche, which is located 27 kms from the center Addis Ababa (Paisa), is located around Akaki area about 7km of East of Tirunesh Beijing Hospital along the road under construction passing the Federal Prison (Kilinto branch), Addis Ababa Science and Technology university (AASTU) and the new Heineken Bear Brewery Factory. It is situated in the South eastern part of Addis Ababa, bounded from east and south by Oromiya region, from west by wereda 05, 08, and 01, and from north by Bole sub city and Oromiya region.

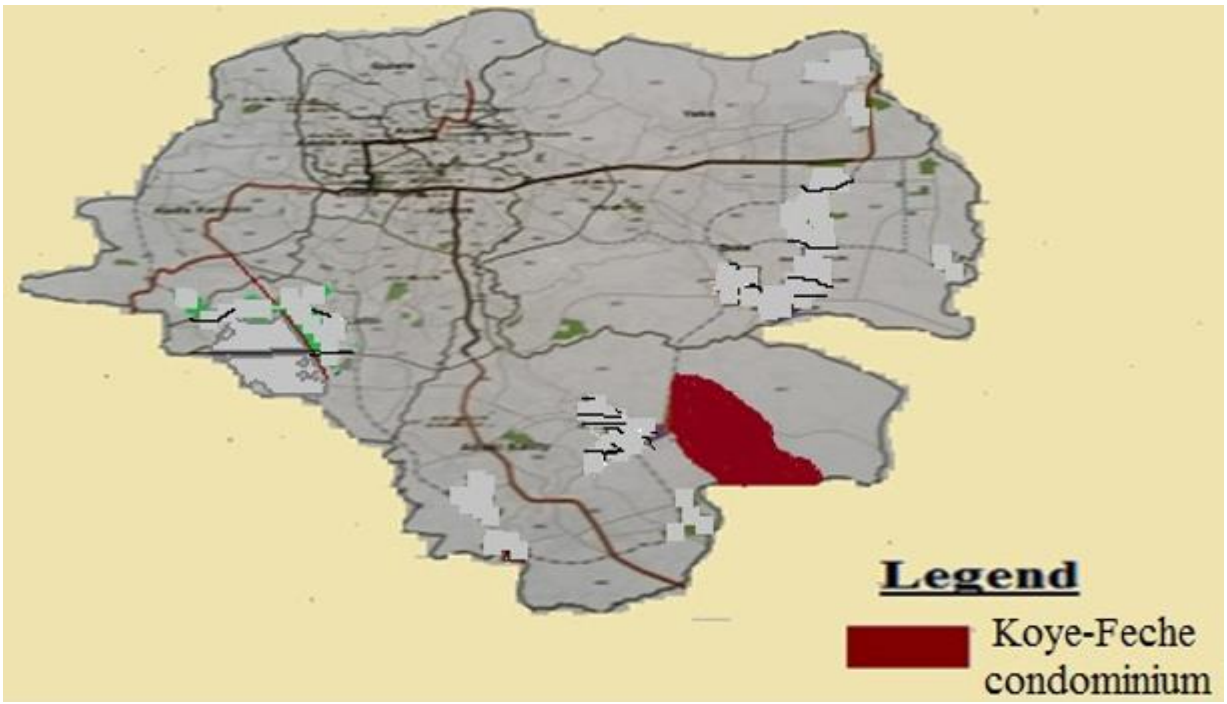

Figure 3.1 Location of Koye-Feche on Addis Ababa city map (Addis Ababa city administration integrated land information center, 2014)

3.1.2. Topography

Koye-Feche is located at 8° 54' 0.00" N latitude and 38° 51' 0.00" E longitude and its altitude is averagely 2,271m (7,454ft) above sea level. However, most of the areas stretch over a predominantly flat land with imperceptible slope changes. There are also scattered and slightly depressed areas which form temporary swamps where rain water settles for short period of time.

3.1.3. Climate

The research area has maximum temperature of 28 °C and the minimum temperature of 4 °C. The weather is usually sunny and dry, but the 'Belg' rains occur from February to April and 'Meher' rains occur from mid-June to mid-September. Generally, the site classified as wet climatic area.

3.1.4. Geological Formation of the Area

The study area is located in southeast Addis Ababa close to Akaki River. According to previous geological studies, the south eastern part of Addis Ababa is covered by volcanic rocks and superficial deposits consisting of the following litho-stratigraphic units from top to bottom.

1. Alluvial and residual soils with varying proportion gravel, sand, silt and clay
2. Trachyte and associated pyroclastic (Yerer Volcanic)
3. Basalt and scoria fallout (Akaki Basic Volcanic)
4. Ignimbrites and variously welded tuffs (Addis Ababa Ignimbrites)

The top part of the sequence is due to fluvial deposition, alteration of the bedrock by combined processes of physical and chemical weathering.

3.2. Data Preparation

3.2.1. Data Collection and Model Input

ANNs learn from examples of data given to them. Thus the first step in creating an artificial neural network was data collection. In this study, secondary data were used for analysis and it was collected from Addis Ababa housing construction office. Addis Ababa housing construction office has conducted soil investigation for Koye-Feche Condominium Building site. The soil investigation was performed at a maximum depth of 10.00m, 12.00m and 15.00 meters below the natural ground surface for G+4 and G+7 buildings.

The collected data constitutes swelling pressure, undrained shear strength, index properties (i.e. atterberg's limit test results, natural moisture content) and dry unit weight. Parameters that are being used to estimate swelling pressure includes liquid limit, plastic limit, moisture content, plasticity index and dry unit weight. Undrained shear strength was predicted using the results of atterbeg's limit test.

3.2.2. Data Filtering

Cluster sampling method (selecting the data with some soil stratification and depth) was utilized to select a suitable data for the proposed ANN based correlation. The soil investigation was conducted for a total of 226 boreholes. However, only 100 boreholes were found appropriate for this particular study. In these boreholes the upper, middle and lower parts of the soil profile were found to mainly contain silty clay and clayey silty sand soil.

Depending on the soil type and depth a total of four datasets has been established for the ANN analysis. Three of the datasets were used to predict undrained shear strength, and the remaining dataset was used to predict swelling pressure. In the first two ANN models of undrained shear strength predictions silty clay soil of depth 1.5 - 2.0m and 3.0 - 5.45m were used. Whereas, the third model utilized clayey silty sand soil with a depth of 1.5m to 5.0m. Additionally, a soil depth of 2.5m to 3.10m was used to develop an ANN prediction model for swelling pressure. The generalized stratification of the soil in the field investigation are divided in to four categories and given below:

Layer 1: soft to medium, highly plastic clay, dark grey with maximum thickness of 2.0m

Layer 2: medium stiff to stiff, silty clay, grayish brown, moist and highly plastic

Layer 3: medium dense to dense, clayey silty sand with gravel light reddish brown

Layer 4: moderately to slightly weathered basalt, light gray

This independent project used a total of 27 and 46 laboratory and field test results of silty clay soils of 1.5m to 2.0m and 1.5m to 5.0m depth, respectively. 61 test results for clayey silty sand soil of 1.5m to 5.0m depth were used to relate the undrained shear strength to the index properties. In addition, 22 laboratory and field tests results had been used to relate the index properties with swelling pressure of fine grained soil (2.50m to 3.10m).

3.3. Development of the ANN Model

3.3.1. Data Preprocessing

Data preprocessing, which is an important step in data mining processes, helps transform the raw data to an understandable format . Thus, examining and preprocessing data before entering the model is essential. Data division, transformation and normalization preprocessing techniques were performed in this study. Loop statements were introduced in matlab to transform and normalize the data. In order to develop the artificial neural network (ANN) model, it is common practice to divide the available data into three subsets.

The data set was divided randomly into three separate data sets - the training data set (70% of the total data set), validation data set (15% of the total data set), and the testing data set (15% of the total data set). The first subset is the training set, which is used for computing the gradient and updating the network weights and biases by repeatedly exposing the network to known input-output data. The error on the validation set is monitored during the training process. The validation error normally decreases during the initial phase of training, as does the training set error. However, when the network begins to over fit the data, the error on the validation set typically begins to rise. The network weights and biases are saved at the minimum of the validation set error. The test set determines how well the model is performing in unknown data. The test set error is not used during training, but it is used to compare different models. It is also useful to plot the test set error during the training process (Hyun II Park a, 2011).

There are four functions provided for dividing data into training, validation and test sets. They are dividerand (the default), divideblock, divideint, and divideind. The data division is normally performed automatically when the network is training. In this study divideind function was used for the data division. It separates targets into three sets: training, validation, and testing, according to indices provided. It actually returns the same indices it receives as arguments; its purpose is to allow the indices to be used for training, validation, and testing for a network to be set manually (Matlab, 2016).

3.3.2. Network Architecture

Because all artificial neural networks are based on the concept of neurons, connections, and transfer functions, there is a similarity between the different structures, or architectures, of

neural networks. The majority of the variations arise from the various learning rules and how those rules modify a network's typical topology (Anderson & McNeill, 1992).

Feedforward, back-propagation architecture is the most popular, effective, and easy to learn model for complex, multi-layered networks. This network is used more than all others combined. It is used in many different types of applications. This architecture has spawned a large class of network types with many different topologies and training methods. Therefore, in this study a back-propagation algorithm was used during training.

The typical back-propagation network has an input layer, an output layer, and at least one hidden layer. Back-propagation algorithm performs gradient background to try to minimize the sum squared error between the network's output values and the known target values. There is no theoretical limit on the number of hidden layers but typically there is just one or two. Some work has been done which indicates that a maximum of four layers (three hidden layers plus an output layer) are required to solve problems of any complexity. Each layer is fully connected to the succeeding layer, as shown in Figure 3.2.

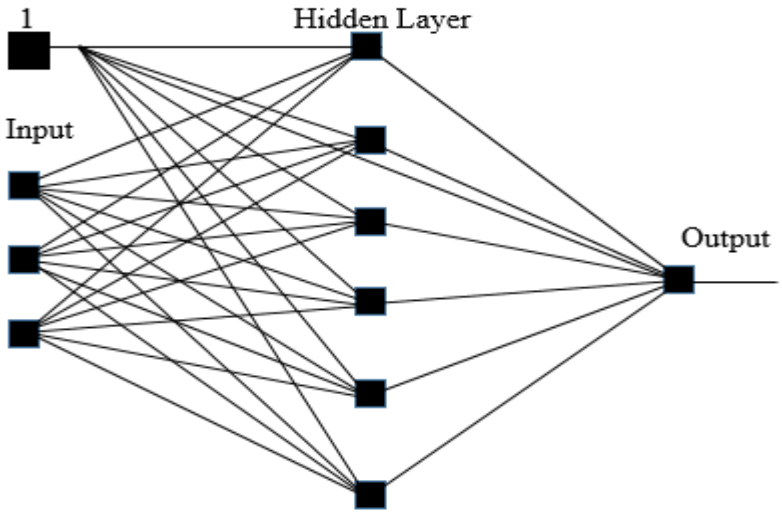

Figure 3.2 Feedforward Back-propagation network

The in and out layers indicate the flow of information during recall. Recall is the process of putting input data into a trained network and receiving the answer. Back-propagation is not used during recall, but only when the network is learning a training set. Conceptually, a network

forward propagates activation to produce an output and it backward propagates error to determine weight changes. The weights on the connections between neurons mediate the past values in both directions.

The number of layers and the number of processing elements per layer are important decisions. These parameters to a feedforward, back-propagation topology are also the most ethereal. They are the "art" of the network designer. There is no quantifiable, best answer to the layout of the network for any particular application (Anderson & McNeill, 1992). However, an attempt was made to easily choose the best layout with the help of loop statements.

Transfer functions calculate layer's output from its net input. They allow ANN to map complex non-linear relationship between input and output. The most common transfer functions are purelin, logsig, and tansig. Each problem has its own best transfer function.

Training function updates weight and bias. Among various training algorithms, Levenberg-Marquardt (trainlm) is recommended for most problems, but for some noisy and small problems Bayesian Regularization (trainbr) can take longer but obtain a better solution. For large problems, however, Scaled Conjugate Gradient (trainscg) is recommended as it uses gradient calculations which are more memory efficient than the Jacobian calculations the other two algorithms use (Matlab, 2016). Every training pattern has its own special characteristics towards the network and differs in simulated results. In any training algorithm, the aim is to reduce the global error. Most learning functions have some provision for a learning rate, or learning constant. Learning rates control the rate of weight adjustment at each step of learning. Usually this term is positive and between zero and one (Anderson & McNeill, 1992).

3.3.3. Network Optimization and Performance

Determining the network architecture is one of the most essential and difficult tasks in ANN model development. It involves the selection of the best number of layers and the number of nodes in each of these. There is no unified approach for determination of an optimal ANN architecture. It is generally, accomplished by fixing the number of layers and choosing the number of nodes in each layer. However, in this research an automated optimization script was written to easily determine the best network architecture.

The performance of the network is the main criteria to choose the best network layout. Accordingly, the best network structure were optimized for various combination of sub-object properties and the best was chosen based on the performance. The correlation coefficient (R) and root mean square error (RMSE) were used to evaluate the performance of the developed ANN model and given in equation (4) and (5).

The correlation coefficient is a statistical measure of the strength of the relationship between two variables. The values range between -1.0 and 1.0. A calculated number greater than 1.0 or less than -1.0 means that there was an error in the correlation measurement. A correlation of -1.0 shows a perfect negative correlation, while a correlation of 1.0 shows a perfect positive correlation. A correlation of 0.0 shows no linear relationship between the two variables. Root mean squared error is the square root of the mean of the square of all of the error. The use of RMSE is very common, and it is considered an excellent general-purpose error metric for numerical predictions (Neill et al., 2018). RMSE is always non-negative, and a value of 0 (almost never achieved in practice) would indicate a perfect fit to the data. In general, a lower RMSE is better than a higher one.

$$\mathrm{RMSE} = \sqrt{\frac{1}{N}\sum_{i=1}^{N}(y_i - y_{j)}{}^2} \tag{4}$$

Where, $N = \text{number of data}$, $y_i = \text{output/predicted}$ $y_j = \text{target/measured}$

$$R = \frac{\sum[(x - \bar{x})(y - \bar{y})]}{\sqrt{\sum(x - \bar{x})^2 * \sum(y - \bar{y})^2}} \tag{5}$$

Where, $y = \text{output or prediction}$ $x = \text{target or observation}$

3.3.4. Mathematical Modeling of Artificial Neuron

A typical structure of ANNs consists of a number of processing elements (PEs), or neurons (nodes), that are usually arranged in layers: an input layer, an output layer and one or more hidden layers (Figure 1).

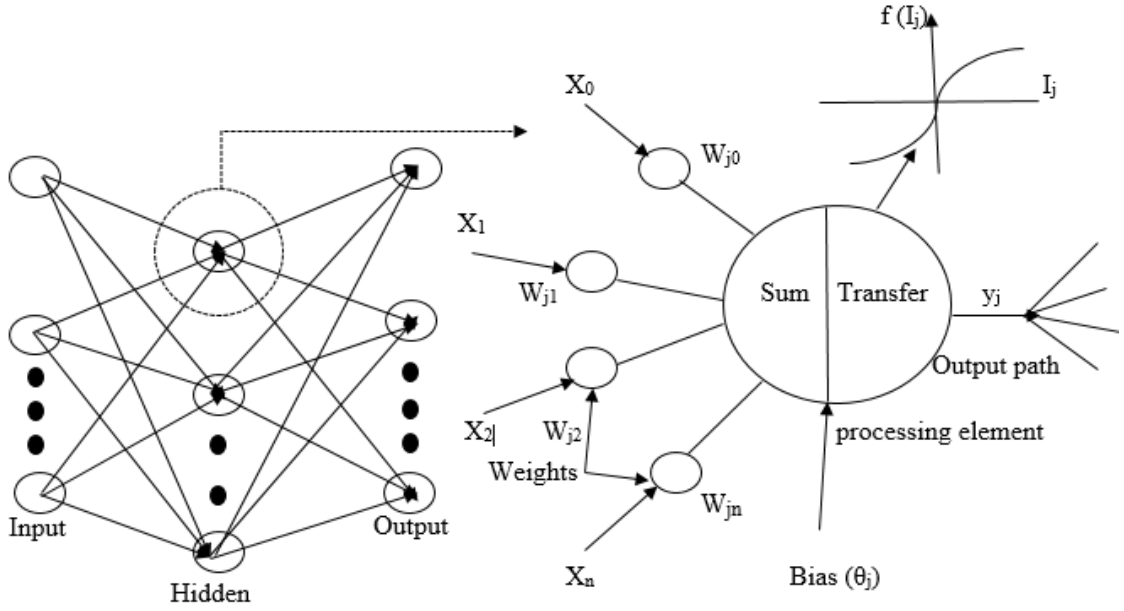

Figure 3.3 Structure and operation of an ANN

Each PE in a specific layer is fully or partially joined to many other PEs via weighted connections. The input from each PE in the previous layer (X_i) is multiplied by an adjustable connection weight (W_{ji}). At each PE, the weighted input signals are summed and a threshold value or bias (θ_i) is added. This combined input (I_j) is then passed through a transfer function ($f(.)$) to produce the output of the PE (y_j). The output of one PE provides the input to the PEs in the next layer. This process is summarized in Equations 1 and 2 and illustrated in Figure 3.3 (Mohamed A. Shahin, 2002)

$$I_j = \sum W_{ji} X_i + \theta_i \quad (6)$$

$$y_j = f(I_j) \quad (7)$$

$$E = \sum_{i=1}^{Num} (T_i - t_i)^2 \quad (8)$$

Where, Num = number of target data, $T_i = i^{th}$ target output $t_i = i^{th}$ calculated output

The propagation of information in ANNs starts at the input layer where the network is presented with a historical set of input data and the corresponding (desired) outputs. The actual output of the network is compared with the desired output and an error is calculated Eq (8). Using this error and utilizing a learning rule, the network adjusts its weights until it can find a set of weights

that will produce the input/output mapping that has the smallest possible error. This process is called “learning” or “training” (Mohamed A. Shahin, 2002).

Once the training phase of the model has been successfully accomplished, the performance of the trained model has to be validated using an independent validation set (Mohamed A. Shahin, 2002).

3.3.5. Workflow of Designing Neural Networks

The main purpose of the research was to predict undrained shear strength and swelling pressure using an artificial neural network. Accordingly, the following procedure had been followed to develop the required model.

1. Access and load the data
2. Preprocess the data
3. Derive features using the preprocessed data
4. Train models using the feature derived in step 3.
5. Iterate to find the best model
6. Integrate the best trained model into a productive system

4. RESULTS AND DISSCUSION

4.1. General

In this section, the findings of the analysis are presented and discussed with regard to the research objective. The study relates the dependent variables (i.e. undrained shear strength and swelling pressure) with the independent variables (i.e. soil index properties). Four different models have been analyzed in the present study with the use of ANN. The first model (Model 1) consists of four inputs $(LL, LL_{mod}, PI, PI_{mod})$ with one output (C_u). The second (Model 2) model consists of five inputs $(LL, LL_{mod}, PI, PI_{mod}, PL)$ with one output(C_u). The third (Model 3) model consists of four inputs $(LL, LI_{mod}, PI, PI_{mod})$ with one output (C_u). The last model consists of five inputs $(LL, W_n, PI, PL, \rho_d)$ with one output (P_s). The data were normalized in the range [0, 1] for analysis. The ANN was implemented using MATLAB 9.0. Two matlab scripts were written for optimization and simulation of the analysis. The first script was used to choose the best network architecture, while the latter was used to develop the final simulation model.

The proposed matlab scripts are given in the Appendix J and Appendix K.

Results of ANN model for the prediction of undrained shear strength and swelling pressure are discussed in section 4.2 and 4.3, respectively. In addition, a comparison of the experimental results of both approaches with some existing and conventional models is also provided in the respective sub-sections.

4.2. Prediction of Undrained Shear Strength using Artificial Neural Network

4.2.1. The Proposed ANN Model for Undrained Shear Strength Estimation

Three prediction models have been developed based on sampling depth and soil type. Input-output correlations were performed in to two phases. Correlation between single input and output variables were established in the first phase. Whereas in the second phase, multiple input variables had been correlated with a single output. For all models the standard two-layer (i.e. single hidden layer and output layer) feed forward network was used.

4.2.1.1. Silty clay soil (at depth 1.5m - 2.0m)

Model 1: The soil parameters used in this model were LL, PI, LL_m, PI_m and C_u. In the first phase a one to one correlation has been established between the dependent variable (C_u) and the independent variables LL, PI, LL_m and PI_m. The second phase was performed by relating all combinations of input parameters with the undrained shear strength.

46 datasets were utilized to develop the neural network prediction model of undrained shear strength for the first phase. The samples were divided in to 3 groups (training, validation and testing). The samples are correlated and the accuracy (comparison between prediction and real data) of each sample is shown in the table below.

Table 4.1 Performance indices for ANN correlation of Cu in phase one (at depth 1.5m – 2.0m)

Variable	N	Transfer Function	Training R	Test R	Validation R	All R
LL Vs Cu	8	logsig-purelin	0.4846	-0.8138	0.5618	0.3179
LLm Vs Cu	49	tansig-purelin	0.3986	0.3810	0.4763	0.3663
PI Vs Cu	46	logsig-tansig	0.4384	-0.3118	0.3275	0.3511
PIm Vs Cu	27	tansig-purelin	0.4731	-0.6384	-0.4662	0.3972

A comparison of experimental results with the results obtained from the ANN model, for training, validation, and testing samples, is depicted in Table 4.1. It can be observed that the performance of the established relation is poor in all cases. However, relatively better performance was obtained when using LL and PIm. In the second phase, the ANN prediction model was developed by combining two input parameters and the resulting model performance is shown in the table below.

Table 4.2 Performance indices for ANN correlation of Cu in phase two (at depth 1.5m – 2.0m)

Variable	N	Transfer Function	Training R	Test R	Validation R	All R
LL, PI Vs Cu	51	tansig-purelin	0.6684	-0.8963	0.5789	0.5371
LLm, PIm Vs Cu	2	logsig-purelin	0.5210	-0.4310	0.9396	0.5310

The results in Table 4.2 show that the neural network model developed in phase 2 produced better prediction performance than phase 1. Thus, for this particular model using combined input parameter yields relatively better prediction of Cu.

The proposed neural network model 1 has one node in the input layer, N nodes in the hidden layer and one node in the output layer. Transfer functions are allocated on the basis of the details presented in the tables. The developed model has been simulated to predict undrained shear strength and the results are tabulated with the corresponding RMSE values as shown in Table 4.3. It can be noted from the table that the performance is lower and unsatisfactory. However, it is possible to improve the performance by adding more training dataset.

Table 4.3 comparison between performance indices of the predicted Cu and experimental results (at depth 1.5m – 2.0m)

Variable	Input data	Output/predicted, Cu	Target/measured, Cu	RMSE
LL	98,100,98,100, 99,104,93	41.27,37.94,41.27, 37.94, 38.99,38.01,29.94	51.6,63.15,43.6, 33.8, 30,34.55,22.7	11.4025
LLm	94.62,92.53,93.06, 95.52, 98.7,93.06,92.68	42.35,40.31,41.02, 42.38, 37.75,41.02,40.52	31.4,42.35,34.65, 61.3,30.05,35.23, 38.8	9.3981
PI	20,44,43,49,43,50, 44	31.25,35.48,30.41, 40.36, 30.41,40.17,35.48	36.3,34.65,33.35, 33.8,30,40.9,24.9	5.2155
PIm	42.19,51.49,53.89, 41.55,27.07,29.01, 24.26	32.62,32.36,30.72, 31.69,35.69,35.13, 36.81	31.4,27.4,27.8, 34.55,36.45,22.7, 42.55	5.7435
LL	68,93,99,108,56,93, 96	40.38,39.77,41.64, 37.28,43.19,34.35, 39.19	36.3,27.4,30.05, 36.15,38.55,22.7, 24.9	9.76
PI	20,44,47,50,21,41, 44			
LLm	94.9,66.77,97.41, 94.57,92.81, 92.68, 98.7	53.67,36.58,34.93, 43.19, 36.56,33.75,35.72	96.78,36.3,33.35, 43.6, 38.55,38.8,37.9	16.45
PIm	43.48,38.35,54.35, 45.4,23.45,39.69, 36.03			

4.2.1.2. Silty clay soil (at depth 3.0m - 5.45m)

Model 2: A dataset containing 27 records was used to develop the model. The analysis was carried out by employing a relation between undrained shear strength and five soil index properties. The correlation was divided into two phases. The first phase of the correlation maps a single input to output relation, while the second phase utilizes combined input parameters.

In phase one each separate network was trained using a single variable as a model input and the relationship is shown in the table below with its corresponding correlation coefficients.

Table 4.4 Performance indices for ANN correlation of Cu in phase one (at depth 3.0m – 5.45m)

Variable	N	Transfer Function	Training R	Test R	Validation R	All R
LL Vs Cu	53	logsig-purelin	0.6232	-0.7309	0.9821	0.7157
PL Vs Cu	60	tansig-purelin	0.9513	0.3694	0.7207	0.3663
PI Vs Cu	37	logsig-purelin	0.9311	-0.9555	-0.7392	0.9066
LLm Vs Cu	58	logsig-purelin	0.9215	-0.7264	-0.9771	0.9072
PIm Vs Cu	45	tansig-tansig	0.5915	-0.7127	0.6836	0.5261

The topology and performance of the networks are shown in Table 4.4. It can be seen from the table that PI and LLm have a strong relationship with undrained shear strength.

The second phase of the correlation was conducted by forming a relationship between combined input variables and undrained shear strength. The performance indices obtained from correlation of combined input parameters are presented in the table below.

Table 4.5 Performance indices for ANN correlation of Cu in phase two (at depth 3.0m – 5.45m)

Variable	N	Transfer Function	Training R	Test R	Validation R	All R
LLm, PIm Vs Cu	32	logsig-purelin	0.8240	-0.9196	0.9446	0.7979
LL, PI Vs Cu	29	logsig-purelin	0.9432	-0.9849	-0.8650	0.8631

As can be seen from Table 4.5 for both correlation combinations, the accuracy of the proposed ANN model has a strong relationship with undrained shear strength. It can be observed from the table that a transfer function combination of tansig/logsig-purelin produces best results.

After the correlation was formed, the next step was to predict the dependent variable (undrained shear strength) using five input variable (predicator) sample data. In Table 4.6, the prediction of undrained shear strength was made and the corresponding performance indices (RMSE) were tabulated. Phase 1 (PI and LLm) indicates very much the best performance results in terms of R and RMSE values. Therefore the undrained shear strength of the silty clay soil for the region considered can be estimated from phase one ANN models. Phase two correlations can also be further improved by increasing the database to achieve the best results.

Table 4.6 comparison between performance indices of the predicted Cu and experimental results (at depth 3.0m – 5.45m)

Variable	Input data	Output/predicted Cu	Target/measured Cu	RMSE
LL	46,67,45,99	29.23,58.98,29.18, 31.46	26.58,96.78,33.4, 46	20.4
PL	35,33,36,29	30.35,28.71,32.96, 33.93	26.58,28.86,33.4, 31.34	2.3
PI	16,16,13,45	32.42,32.41,31.11, 33.92	38.64,30.9,40.24, 31.4	5.72
LLm	51.61,36.66, 10.56,29.61	26.66,29.15,36.99, 29.53	29.22,33.73,39.76, 33.4	3.54
PIm	10.1,16.9,26.8, 44.6	44.92,32.28,38.56, 45.41	40.24,33.63,28.8, 39.45	6.19
LLm	59.36,17.91, 52.74,18.8	80.87,35.64,48.19, 36.69	96.78,26.37,24.37, 31.34	15.28
PIm	35.4,13.7,36.9, 13.6			
LL	37,55,56,33	35.27,44.30,33.43, 29.82	40.24,18.68,30.98, 39.76	14.02
PI	13,24,19,6			

4.2.1.3. Clayey silty sand soil (at depth 1.5m - 5.0m)

Model 3: The database used for this model consists of 61 datasets. Seventy percent of the data was used for training purposes and the remaining 30 % was used to validate and test the model's performance. The correlation was performed in two phases. In the first phase, the input variables LL, PI, LLm and PIm were used to correlate with undrained shear strength. In addition, the combination of these parameters has been used in the second phase. The resulting artificial neural network model with the corresponding performance indices for both phases are shown in the tables given below.

Table 4.7, presents the model developed in phase one with the corresponding correlation coefficient, R. The relationship between PI and PIm with undrained shear strength provides comparatively better performance. It can be noted from the table that a combination of sigmoid and linear transfer function yields better results.

Table 4.7 Performance indices for ANN correlation of Cu in phase one (at depth 1.5m – 5.0m)

Variable	N	Transfer Function	Training R	Test R	Validation R	All R
LLm Vs Cu	39	logsig-purelin	0.4393	-0.5548	0.7017	0.3149
LL Vs Cu	29	tansig-purelin	0.5177	0.360	0.7472	0.3922
PI Vs Cu	55	tansig-purelin	0.3425	0.6195	0.9086	0.4152
PIm Vs Cu	44	tansig-purelin	0.4833	0.6973	0.8455	0.5309

The correlation between the relationship of the combined input parameters with undrained shear strength and the corresponding performance for phase two is shown in Table 4.8. The model employed from combined input parameters relatively yields better results than phase one correlations.

Table 4.8 Performance indices for ANN correlation of Cu in phase two (at depth 1.5m – 5.0m)

Variable	N	Transfer Function	Training R	Test R	Validation R	All R
LLm, PIm Vs Cu	44	tansig-purelin	0.4833	0.697	0.8455	0.531
LL, PI Vs Cu	60	tansig-purelin	0.5238	0.583	0.8899	0.524

Prediction of undrained shear strength was made using all developed ANN models and corresponding performance indices (RMSEs) were given in Table 4.9. The prediction was made using nine datasets. From the table it can be noted that the model developed using combined input variables (liquidity index and plasticity index) produced good performance in terms of both RMSE and R. Thus, undrained shear strength for the area considered in this model can be estimated with acceptable accuracy using the developed ANN (LI and PI) model.

Table 4.9 comparison between performance indices of the predicted Cu and experimental results (at depth 1.5m – 5.0m)

Variable	Input data	Output/predicted Cu	Target/measured Cu	RMSE
LLm	14.21,41.92,43.3, 28.77,36.67,33.3, 46.67,47.95,39.44	37.28,34.98,35.13,49.01, 39.71,36.13,47.19,56.05, 39.4	40.5,33.35,30.05, 44.55,43.6,27.8, 48.01,42.55,36.55	6.0945
LL	87,94,97,93, 89,92,86,92,93	36.68,37.33,39.53,36.88, 36.33,36.56,36.96,36.56, 36.88	34.65,60.6,63.15, 30.05,35.65,37.6, 53.3,37.5,36.55	12.56
PI	41,45,41,30,47, 41,42,47,44	37.29,40.07,37.29,47.56, 41.21,37.29,38.32,41.21, 39.62	35.65,40.9,39.15, 53.3,48.01,37.5, 43.05,42.1,42.55	3.617
PIm	86.65,70.79,95.81, 80.35,96.22,83.83 ,87.84,91.42,91.69	39.28,38.36,40.27,38.79, 40.32,39.04,39.39, 39.76,39.79	42.35,34.95,33.35, 44.55,34.55,35.23, 37.4,37.9,36.55	4.3186
LLm	88.38,94.24,95.52, 69.06,103.27,89.52, 90.18,95.93,95.81	38.01,37.65,40.37,52.35, 52.48,38.61,37.35,40.99, 38.47	35.65,40.9,39.15, 53.3,48.01,37.5, 43.05,42.1,42.55	3.16
PIm	40.71,44.64,40.8, 24.1,6.67,39.89, 41.62,46.48,43.91			
LL	98,81,92,84,87,104, 92,96,90	39.55,43.28,35.48,34.86, 34.62,46.74,36.86,39.78, 36.03	35.7,44.55,37.6, 35.23,36.45,48.01, 38.8,38.2,37.5	1.95
PI	45,29,42,39,40,47, 44,46,43			

4.2.2. Comparison of ANN Model with the Conventional Regression Analysis

Artificial neural networks do not require any prior knowledge of the existence of the relationship between input/output variables, which is one of the advantages that ANNs have compared to statistical and other approaches. In this section, an attempt has been made to assess the relative performance of ANNs over the conventional method. The results obtained using the neural network were compared with the results of the traditional method. For the conventional method, excel tool was used to establish a relationship between the input/output variables.

The graph established for regression analysis of undrained shear strength are given in the Appendix F, Appendix G and Appendix H.

The two methods were compared as shown in table 4.10, 4.11 and 4.12.

Table 4.10 comparison between ANN model with conventional regression analysis (model-1)

Variable	N	Transfer Function	All R	Regression Analysis RA
LL Vs Cu	8	logsig-purelin	0.3179	0.2487
PI Vs Cu	46	logsig-tansig	0.3511	0.2009
LLm Vs Cu	49	tansig-purelin	0.3663	0.2014
PIm Vs Cu	27	tansig-purelin	0.3972	0.2672
LL, PI Vs Cu	51	tansig-purelin	0.5370	0.2272
LLm, PIm Vs Cu	2	logsig-purelin	0.5310	0.0251

Table 4.11 Comparison between ANN model with conventional regression analysis (model-2)

Variable	N	Transfer Function	All R	Regression Analysis RA
LL Vs Cu	53	logsig-purelin	0.7157	0.6335
PL Vs Cu	60	tansig-purelin	0.3663	0.4364
PI Vs Cu	37	logsig-purelin	0.9066	0.8199
LLm Vs Cu	58	logsig-purelin	0.9072	0.7904
LL, PI Vs Cu	29	logsig-purelin	0.8631	0.2519
LL, PI Vs Cu	60	tansig-purelin	0.5238	0.583

Table 4.12 Comparison between ANN model with conventional regression analysis (model-3)

Variable	N	Transfer Function	All R	Regression Analysis RA
LLm Vs Cu	39	logsig-purelin	0.3149	0.2998
LL Vs Cu	29	tansig-purelin	0.3922	0.3578
PI Vs Cu	55	tansig-purelin	0.4152	0.2687
PIm Vs Cu	44	tansig-purelin	0.5309	0.4104
LLm, PIm Vs Cu	44	tansig-purelin	0.531	0.2
LL, PI Vs Cu	60	tansig-purelin	0.524	0.176

In the above tables, regression analysis was carried out to obtain the coefficients of correlation of predicted versus measured results for neural networks and the traditional methods. It is evident from the tables that the ANNs outperform the conventional method which indicates that the ANN model has relatively a higher predictive accuracy than the RA model.

4.2.3. Comparison of ANN model with Previously Developed Correlations

This section compares the performance of the experimental results of ANNs with some existing models. A total of 46 datasets were used for the analysis. The developed ANNs model by using these data was compared with available literature studies. In order to compare the performance of equations developed by Lee (2004), Berligen et al. (2007) and Vardanega and Haigh (2017) with ANNs, correlation coefficient (R) and root mean square error (RMSE) term were utilized.

Table 4.13 shows a comparison of the performance of the ANNs with previously developed empiric formulas based on laboratory experiments. It can be seen from the table that the ANNs model relatively performs well, as it has high correlation coefficients, r, and low root mean squared errors (RMSE) between the measured and predicted undrained shear strength compared to the three empiric equations.

Table 4.13 Comparison between ANN model with some existing empirical equations of Cu

Source	Relationship	Model	Data set use		R	RMSE
			All	46	0.4538	
	Cu Vs LL, Wn	ANN	Training	32	0.5853	7.86
			Validation	7	0.5446	
			Test	7	0.4251	
Lee, 2004	$Cu = 182.93e^{(-2.3714*\frac{Wn}{LL})}$	MRA	46		0.0424	33.034
Berligen et al., 2007	$Cu = 145e^{(-2.86*\frac{Wn}{LL})}$	MRA	46		0.0436	20.19
Vardanega and Haigh, 2017	$Cu = 10^{(2.72-2.585(\frac{Wn}{LL}))}$	MRA	46		0.0458	43.107

4.3. Prediction of Swelling Pressure using Artificial Neural Network

4.3.1. The Proposed ANN Model for Swelling Pressure Estimation of fine grained soil

4.3.1.1. Fine grained soil

Model 4: The ANN model was designed to predict swelling pressure from LL, PI, PL, ρ_d and Wn. A total of 22 datasets had been used to develop the model. The swelling pressure was correlated to input variables in to two phases. Phase one comprises a one to one input-output correlation. Whereas in the second phase, multiple inputs were correlated with the swelling pressure.

The relationship established in the first phase and the resulting performance of the NN analysis are shown in the table below.

Table 4.14 Performance indices for ANN correlation of Ps in phase one

Variable	N	Transfer Function	Training R	Test R	Validation R	All R
LL Vs Ps	30	tansig-purelin	0.4132	0.5812	0.9999	0.4504
PI Vs Ps	50	logsig-purelin	0.6907	-0.522	0.8425	0.6056
PL Vs Ps	36	tansig-tansig	0.4803	0.2915	0.9889	0.5464
ρ_d Vs Ps	56	tansig-purelin	0.6044	0.9908	0.9998	0.7153
Wn Vs Ps	23	logsig-logsig	0.7133	-0.7715	0.9151	0.6449

Table 4.14 shows that the ANN model established from plasticity index, dry unit weight and moisture content, has a relatively strong relationship with swelling pressure. It can be noted from the table that Ps values obtained from the ANN model of dry unit weight and plasticity index correlations are in good agreement with the experimentally obtained (target) Ps values for sigmoid-linear function. On the other hand, the ANNs correlation of natural moisture content with sigmoid-sigmoid transfer function produces better results.

Table 4.15 depicts that the ANNs correlation of combined input parameters with swelling pressure of the second phase and the corresponding performance indices.

Table 4.15 Performance indices for ANN correlation of Ps in phase two

Variable	N	Transfer Function	Training R	Test R	Validation R	All R
ρ_d, Wn Vs Ps	49	tansig-purelin	0.7748	0.8951	0.9626	0.8346
ρ_d, PLVs Ps	39	tansig-purelin	0.7811	0.9299	0.7421	0.7256
ρ_d, Wn, LL Vs Ps	32	tansig-purelin	0.9454	0.9697	0.8739	0.9041
ρ_d, Wn, PI Vs Ps	60	tansig-purelin	0.8458	0.9527	0.9964	0.8576
ρ_d, Wn, PL Vs Ps	24	logsig-purelin	0.887	0.9955	0.9903	0.8639
ρ_d, Wn, LL, PI Vs Ps	39	tansig-purelin	0.864	0.9761	0.8475	0.8129
LL, PI, PL Vs Ps	10	logsig-purelin	0.6929	0.8615	0.9989	0.701
ρ_d, LL, PI, PL Vs Ps	37	tansig-purelin	0.9083	0.9082	0.6321	0.7955
Wn, LL, PI, PL Vs Ps	37	tansig-purelin	0.7319	0.9519	0.8602	0.6419
ρ_d, Wn, LL, PI, PL Vs Ps	56	logsig-purelin	0.9085	0.9797	0.9864	0.9342

As it can be seen in the above table the ANN model developed using input variables of ρ_d, Wn, LL, PI and PL shows strong relationship with swelling pressure. It can also be noted that sigmoid-linear transfer function produces relatively best results. In addition, ANN model designed using the input parameters of ρ_d, Wn and LL with a sigmoid-linear transfer function is also in good agreement with the experimental value of swelling pressure. In general, it can be deduced that ANN model formed in the presence of both dry unit weight and natural moisture content shows a soundly relationship with swelling pressure.

After making ANN based correlation and finding best performance the next step was predicting the dependent variable (swelling pressure) using five input (predicator) sample data. Accordingly, the predicted swelling pressure is tabulated in Table 4.16 and 4.17 along with the performance indices. It can be noted from the table that the ANN based correlation formed using ρ_d, Wn, LL, PI and PL produces best Ps prediction results. Thus, the developed ANN model can be used to predict swelling pressure with a higher accuracy.

Table 4.16 comparison between performance indices of the predicted Ps and experimental results -1

Variable	Input data	Output/predicted (Ps)	Target/measured (Ps)	RMSE
ρ_d	98,87,88	32.39,36.39,38.25	30.1,34.3,36.3	2.11
Wn	48,52,53	41.22,34.64,31.19	43.7,28.6,32.1	3.807
LL	46,33,41	30.19,35.66,39.2	30.2,35.5,41.3	1.2137
PI	11.23,12.79,13.08	30.66,39.69,14,43.28	25.5,35.5,39.8	4.3305
PL	46.54,32.57,49.93	35.63,35.64,35.67	30.1,35.7,39.4	3.8506
ρ_d	12.68,11.24, 12.79	31.32,27.005,36.302	30.1,28.6,35.5	1.2489
Wn	46.54,30.61,43.01			
PL	39,41,33	40.71,40.18,38.05	42.3,49.6,35.5	5.7097
ρ_d	12.35,12.56,12.79			
LL	87,93 96	39.23,42.89,37.49	34.3,49.6,37.3	4.8082
ρ_d	12.46,12.56, 11.78			
Wn	48.25,36.44, 35.47			
PI	47, 52, 49	39.44,43.78,36.82	42.3,49.6,36.3	3.7534
ρ_d	12.35,12.56,36.44			
Wn	40.86,11.58,42.25			
PL	39,45,47	43.44, 29.45,38.42	42.3,32.1,37.4	1.7649
ρ_d	12.35,10.44,12.45			
Wn	40.86,49.49,38.85			
LL	71, 88, 97	26.19,39.81,40.71	35.5,36.3,37.4	6.0491
PI	38, 12.79,43.01			
ρ_d	49, 11.58,42.25			
Wn	52, 12.45,38.85			

Table 4.17 Comparison between performance indices of the predicted Ps and experimental results-2

Variable	Input data	Output/predicted (Ps)	Target/measured (Ps)	RMSE
LL	96, 97, 95	33.95,33.31,49.17	37.3,37.4,45.3	3.7838
PI	51,52,54			
PL	45,47,40			
ρ_d	12.56,11.42,12.45	38.89,38.81,28.85	49.6,39.4,37.4	7.92
LL	93,92,97			
PI	52,49,52			
PL	41,43,47			
Wn	36.44, 49.93, 38.85	40.97,33.03,36.02	49.6,39.4,37.4	6.2449
LL	93,92,97			
PI	52,49,52			
PL	41,43,47			
Wn	35.35 , 36.44, 42.25	26.83,50.48,37.71	30.2,49.6,36.3	2.1672
ρ_d	11.3,12.56,11.58			
LL	98,93,88			
PI	52,52,49			
PL	46,41,39			

4.3.2. Comparison of ANN Model with the Conventional Regression Analysis

Correlations can be made in various ways. Regression analysis is one of the commonly used and the easiest conventional method of setting up a correlation. However, in this study an effort was made to establish ANN model with a relatively higher accuracy. Accordingly, the developed was compared with the conventional regression analysis and the performance indices are shown in Table 4.18. From the table, it is found that the values predicted from the ANN

models much better matched to the experimental values than those obtained from the RA models.

The graph established for regression analysis of swelling pressure are given in the appendix I

Table 4.18 Comparison between Ps ANN model with the conventional regression analysis

Variable	N	Transfer Function	All R	Regression Analysis (RA)
LL Vs Ps	30	tansig-purelin	0.4504	0.4055
PI Vs Ps	50	logsig-purelin	0.6056	0.4587
PL Vs Ps	36	tansig-tansig	0.5464	0.5387
ρ_d Vs Ps	56	tansig-purelin	0.7153	0.6023
Wn Vs Ps	23	logsig- logsig	0.6449	0.6241
ρ_d, Wn Vs Ps	49	tansig-purelin	0.8346	0.2836
ρ_d, PLVs Ps	39	tansig-purelin	0.7256	0.3786
ρ_d, Wn, LL Vs Ps	32	tansig-purelin	0.9041	0.2865
ρ_d, Wn, PI Vs Ps	60	tansig-purelin	0.8576	0.3003
ρ_d, Wn, PL Vs Ps	24	logsig- purelin	0.8639	0.3787
ρ_d, Wn, LL, PI Vs Ps	39	tansig-purelin	0.8129	0.3847
LL, PI, PLVs Ps	10	logsig- purelin	0.701	0.3905
ρ_d, LL, PI, PLVs Ps	37	tansig-purelin	0.7955	0.5067
Wn, LL, PI, PLVs Ps	37	tansig-purelin	0.6419	0.3909
ρ_d, Wn, LL, PI, PLVs I	56	logsig- purelin	0.9342	0.5327

4.3.3. Comparison of ANN model with Previously Developed Correlations

Table 4.19 shows the comparison between the developed ANN model and some existing empirical equations. Three previously formulated equations were selected for comparison. The selection criteria was based on the soil type and the relative proximity to the experimental results. The empirical equations and ANNs with the respective performance indices are tabulated in the table below.

It can be observed from the table that the ANN model yields better matching results with the experimentally obtained swell pressure values, as compared to those obtained by using previous empirical equations.

Table 4.19 Comparison between ANN model with some existing empirical equations of Ps

Model		ANN		RA	
Source	Relationship	Data set use			
		All	22	22	
		Training	16		
		Validation	3		
		Test	3		
		R	RMSE	R	RMSE
Vijayavergiya & Ghazzaly, 1973	$\log Ps = \frac{1}{12}(0.4LL - Wn + 23.6)$	0.7599 0.8576 0.9653 -0.9872	8.32	0.1683	312.33
Erguler and Ulusay, 2003	$Ps = 3.02PI - 48.13$	0.5754 0.6002 0.989 -0.964	4.28	0.0128	62.63
Asamnew G., 2016	$Ps = 1.5197 * \gamma_d + 0.3042PI - 31.4295$	0.7629 0.8043 0.9914 -0.8262	5.02	0.2905	127.56

5. CONCLUSION AND RECOMMENDATION

5.1. Conclusion

The purpose of the research was to develop an artificial neural network model that can be employed for predicting undrained shear strength and swelling pressure of fine grained soil. MATLAB 9.0 software was used to build an artificial neural network model. Two types of Matlab scripts have been written to be used for optimization and simulation of the network. The first script was used to pick the best network architecture and the second script was used to simulate the model. Thus, artificial neural network model has been developed which gave reasonably acceptable results. Accordingly, four ANN models were proposed depending on soil type and sampling depth. In addition, the ANN model was compared with conventional regression analysis and previous empiric formulas.

The following conclusions were drawn from the research:

- The proposed ANN model can predict undrained shear strength and swelling pressure with quiet efficient accuracy.
- ANN model was compared with the conventional regression analysis and found superior in all cases.
- The results obtained from ANN and existing empirical formulas were compared to those obtained from the experiments. It was found that the values predicted from the ANN models match the experimental values much better than those obtained from the equations.
- An automated optimization script has been developed that can be successfully used to pick the optimal network architecture.
- Sigmoid-linear transfer function performed the best among the various combinations and was able to predict undrained shear strength and swelling pressure on fine grained soil closer to the actual one.

5.2. Recommendation

- Using trained ANN structures as an inexpensive substitute for laboratory research, the undrained shear strength and swell pressure of fine grained soils included in this study could be predicted quite easily and efficiently.
- By further increasing the database even better prediction performance can be achieved.
- The developed artificial neural network can be applied for other geotechnical predictions with minimum effort.

REFERENCES

Agrawal, G., Chameau, J. A., & Bourdeau, P. L. (1997). Assesing the Liquifaction Susciptibility at a Site Based on Information from Penetration Testing. *In: Artificial Neural Networks for Civil Engineers: Fundamentals and Applications.* Newyork: N. Kartam, I. Flood & J. H. Garrett, Eds.

Ajayi, L. A., & Balogun, L. A. (1988). Penetration Testing in Tropical Lateritic and Residual Soils- Nigerian Experience. *Penetration Testing*, 315-328.

Anderson, D., & McNeill, G. (1992). *Artificial Neural Network Technology.* Newyork: Kaman Sciences Corporation.

Alemayehu Teferra,& Mesfin, L. (1999). *Soil Mechanics.* Addis Ababa: A. A. U. Printing Press.

Asaminew,G. (2016). *Developing Correlation Between Index Properties and Swelling Potential of The Expansive Soils Found in Woliso Town.* Addis Ababa: Addis Ababa University, MSc. Thesis.

Ashenafi, T. (2013). *Study on Index Properties and Swelling Pressure of Expansive Soils Found in Dukem.* Addis Ababa: Addis Ababa University, MSc. Thesis.

Barakat, S., & Attom, M. F. (1999). Comparison Between Multiple Regression Analysis and Artificial Neural Networks in Evaluating Swelling Pressure of Clayey Soils Using Three Methods. *Journal of the Institute of Engineers. Civil Engineering Division*, 86-93.

Bowles, J. E. (1996). *Foundation Analysis and Design, 5th Edition.* McGraw-Hill Companies, Inc. : Newyork.

Budhu, M. (2015). *Soil Mechanics Fundamentals.* Newyork: John Wiley and Sons Ltd.

Dagnachew, T. (2003). *Examining the Swelling Pressure of Addis Ababa Expansive Soil.* Addis Ababa: Addis Ababa University, MSc. Thesis.

Decourt, L. (1990). *The Standard Penetration Test.* Oslo: State of the Art of Report, Norwegian Geotechnical Institute Publication.

Dhowian, A., Erol, A. O., & Abdulfattah, Y. (1998). *Evaluation of Expansive Soil and Foundation Methodology in the Kingdom of Saudi Arabia* . Riyadh: King Abdulaziz for Science and Technology.

Douglas, C. M., & George, C. R. (2003). *Applied Statistics and Probablity for Engineers, Third Edition.* Newyork: John Wiley and Sond,Inc.

Edy Tonnizam and Danial Johad. (2014). prediction of swelling pressure using artificial neural networks.

Elias A. (2012). *Prediction of Swelling Behaviour of Addis Ababa Expansive Soil Using Simple Mathematical Model.* Addis Ababa: Addis Ababa University, MSc. Thesis.

Elshorbagy, A., Corzo, G., Srinivasulu, S., & Solomatine, D. P. (2010). *Experimental Investigation of the Predictive Capabilities of Data Driven Modelling Techniques in Hydrology-Part 1: Concepts and Methodology.* Hydrology and Earth System Science.

Elshorbagy, Corzo, Srinivadulu and Solomatine. (2010). *state of the art of artificial neural network in geotechnical enginnering.*

Erzin, Y. (1997). *Swell Pressure Soil Suction Relationships.* Ankara: University of Middle East Technical, MSc. Thesis.

Erzin, Y. (2008). The Use of Artificial Neural Network for the Prediction of Swell Pressures. *The 12th International Conference of IACMAG*, (pp. 957-965). Goa, India.

Erzin, Y., & Erol, O. (2004). Correlation for Quick Prediction of Swell Pressures. *The Electronic Journal of Geotechnical Engineering*.

Erzin, Y., & Gunes, N. (2011). The Prediction of Swell Percent and Swell Pressure by Using Neural Networks. *Mathematical and Computational Applications*, 425-436.

Farrokhzad, cheobasti and Barari. (2010) from index properties prediction of free swell .

Farrokhzad, F., Choobasti, A. J., & Barari, A. (2010). Artificial Neural Network Model for Prediction of Liquifaction Potentials in Soil Deposits. *5th International Conference of*

Recent Advances in Geotechnical Earthquake Engineering and Soil Dynamics (pp. 1-8). Missouri: Missouri University of Science and Technology.

Fratta, D., Aguettant, J., & Smith, L. R. (2007). *Introduction to Soil Mechanics Laboratory Testing.* Washington DC.: Tylor and Francis Group.

Goh, A. T. (1995a). Back Propagation Neural Networks for Modelling Complex System. *Artificial Intelligence in Engineering, 9*(3), 141-151.

Hafez, D. H., Mahgoub, A. G., & Kiefa, M. A. (2017, January). General Regression Neural Network Modelling of Soil Characeristics from Field Tests. *International Journal of GEOMATE, 12*(29), 132-139.

Hara, A., Ohta, T., Niwa, M., Tanaka, S., & Banno, T. (1974). Shear Modulous and Shear Strength of Cohesive Soils. *Soils and Foundation, 14*(3), 1-12.

Haryana. (2017). the state of artificial neural networks in geotechnical engineering.

Hettiarachchi, H., & Brown, T. (2009). Use of SPT Blow Counts to Estimate Shear Strength Properties of Soils: Energy Balance Approach. *Journal of Geotechnical and Geoenvironmental Energy, 135*(6).

Jibanchand. (2017) The Standard Penetration Test in Insensetive Clays and Soft Rock. *Proceeding of the 1st European Symposium on Penetration Testing*.

Kebede, A. (2016). *Correlation Between Standard Penetration Test with Unconfined Strength and Index Property of Fine Grained Soil.* Addis Ababa: Addis Ababa University, MSc. Thesis.

Kemal, A. (2015). *Correlation Between Index Properties and Swelling Pressure of Expansive Soils Found Around Koye Area.* Addis Ababa: Addis Ababa University, MSc. Thesis.

Kolay, P. K., Bustami, R. A., & Shirley, Y. (2011). Prediction of Compression Index for Tropical Soil by Using Artificial Neural Network. *13th International Conference of the IACMAG* (pp. 542-547). Melbourne: Researchgate.

Komornik, A., & David, D. (1969). Prediction of Swelling Pressure of Clays. *Journal of Soil Mechanics and Foundation Engineering Division, ASCE, 95*(1), 209-225.

M. A. Shahin, M. B., & Maier, H. R. (2008). State of The Art of Artificial Neural Networks in GEotechnical Engineering. *EJGE*, 1-26.

Mengistie, A. (2014). *Correlation Between Index Properties and Swelling Characteristics of Expansive Soil (The Case of Asella Town).* Addis Ababa: Addis Ababa University, MSc. Thesis.

Meulenkamp and Grima. (1999).Applicability of Standard Penetration Tests To Estimate Undrained Shear Strength of Soils of Imphal

Mitcell, J. K., Guzikowski, F., & Villet, W. C. (1978). *The Measurement of Soil Properties In-Situ- Present Methods-Their Applicability and Potential.* Department of Civil Engineering. California: University of California.

Mitchell, J. K. (1976). *Fundamentals of Soil Behaviou.* Newyork: McGraw-Hill Companies, Inc.

Naijar, Y. M., Basheer, I. A., & McReynolds, R. (1996). *Neural Modelling of Kansas Soil Swelling.* Kansas: Transportation Research Record.

Nassaji, F., & Kalantari, B. (2011). SPT Capability to Estimate Undrained Shear Strength of Fine-Grained Soils of Tehran, Iran. *Electronic Journal of Geotechnical Engineering*, 1229-1238.

Nayak, N. V., & Christensen, R. W. (1974). Swelling Characteristics of Compacted Expansive Soils. *Clay and Clay Minerals, 19*(4), 251-261.

Niguusie, D. (2007). *Indepth Investigation of Relationship Between Index Property and Swelling Characteristics of Expansive Soil in Bahirdar.* Addis Ababa: Addis Ababa University, MSc. Thesis.

Nova, R. (2010). *Soil Mechanics: Fundamentals of Soil Behaviour* . Newyork: John Wiley and Sons, Inc.

Park, H. I. (2011, April 11). Study for Application of Artificial Neural Networks in Geotechnical Problems. Shangahi, China: Artificial Neural Networks-Application,Dr. Chi Leung Patrick Hui (Ed). Retrieved from http://www.intechopen.com/books/artificial-neural-networks-in-geotechnical-problems

Parry, R. H. (1977). Estimating Bearing Capacity of Sand from Standard Penetration test Values. *JGED, ASCE*, 1013-1045.

Sanglerat, G. (1972). *The Penetration and Soil Exploration Interpretation of Penetration Diagrams: Theory and Practice.* Amsterdam: Elsevier Publishing Co.

Seed, H. B., Woodward, R. J., & Lundgren, R. (1962). Prediction of Swelling Potential for Compacted Clays. *Journal of The soil Mechanics and Foundation Division, ASCE, 88*, 107-131.

Singh, N. B., Jibanchand, N., & K. R, D. (2017). Applicability of Standard Penetration Tests To Estimate Undrained Shear Strength of Soils of Imphal. *International Journal of Engineering Technlology, Science and Research, 4*(3), 250-255.

Sirvikaya, O. (2009). Comparison of Artificial Neural Network Models With Correlative Works on Undrained Shear Strength. *Eurosian Soil Science, 24*(13), 1487-1496.

Sowers, G. F. (1979). *Introductory Soil Mechanics and Founadtions, 4th Edition.* Newyork: Mcmillan.

Specht, D. F. (1991). A General Regression Neural Network. *IEEC Trans. Neural Networks*, *2*, pp. 568-576.

Sridharan, A. (1990). Engineering Behaviour of Fine Grained Soils: A Fundamental Approach . *13th IGS Annual Lecture Delivered on the Occasion of its 32nd Annual General Session*, (pp. 447-540). Bombay.

Stroud, M. A. (1974). The Standard Penetration Test in Insensetive Clays and Soft Rock. *Proceeding of the 1st European Symposium on Penetration Testing*, *2*, pp. 367-375. Stockholm.

Terzaghi, K., & Peck, R. B. (1967). *Soil Mechanics in Engineering Practice.* Newyork: John Wiley.

Terzaghi, K., Peck, R. B., & Mesri, G. (1996). *Soil Mechanics in Engineering Practice: Third Edition.* Newyork: John Wiley and Sons.

Vijayavergiya, V. N., & Ghazzaly, O. (1973). Prediction of Swelling Potential for Natural Clays. *Proceeding of 3rd International Conference on Expansive Soils*, (pp. 227-236). Haifa.

Wasserman. (1989) General Regression Neural Network Modelling of Soil Characeristics from Field Tests.

Zewdie, A. (2004). *Investigation in to Shear Strength Characteristics of Expansive Soil of Ethiopia.* Addis Ababa: Addis Ababa University, MSc. Thesis .

APPENDICES

Appendix A Coordinate and depth of boreholes

Sr. No.	BH-ID	Easting	Northing	Elevation (m.a.s.l)	Depth drilled (m)
1	BH-53	480131.2	984563.2	2187	10
2	BH-54	480136.8	984592.4	2189	10
3	BH-55	480134.3	984613.3	2189	10
4	BH-56	480138.2	984635.1	2190	10
5	BH-57	140480.4	984654.7	2191	10
6	BH-58	480143.2	984684.6	2191	10
7	BH-59	480149.5	984711.6	2193	10
8	BH-60	480150.8	984730	2194	10
9	BH-61	480157.1	984755.7	2196	10
10	BH-62	480186.2	984776.1	2197	10
11	BH-63	480177.1	984605.4	2189	10
12	BH-64	480181.8	984633.9	2191	10
13	BH-65	480203.5	984602.7	2189	10
14	BH-66	480207.8	984630.8	2190	10
15	BH-69	480233.8	984610.3	2190	12
16	BH-70	480237.9	984636.8	2191	15
17	BH-71	480237.9	984674.9	2193	12
18	BH-72	480246.9	984701.1	2194	12
19	BH-73	480250.8	984734	2195	12
20	BH-74	480255.1	984762.2	2197	15
21	BH-75	480096.5	984840.6	2199	10
22	BH-76	480120	984837.6	2199	10
23	BH-77	480146.5	984828.8	2199	10
24	BH-78	480167.7	984828.8	2199	10
25	BH-79	480188.7	984825.8	2199	10
26	BH-80	480129.4	984862.8	2200	10
27	BH-81	480132.6	984891.7	2201	10
28	BH-82	480189.3	984854	2200	10
29	BH-83	480194	984882	2201	10
30	BH-84	480096.2	984872.7	2199	10
31	BH-85	480070	984875.6	2199	10
32	BH-86	480076.8	984927.5	2200	10
33	BH-87	480103.8	984925.5	2201	10
34	BH-88	480131.5	984920.8	2201	10
35	BH-89	480158.4	984917.3	2201	10

36	BH-90	480184.3	984916.2	2201	10
37	BH-91	480207.5	984913.7	2201	10
38	BH-92	480228.2	984908.5	2201	10
39	BH-93	480037.5	984877.6	2198	15
40	BH-94	480021.4	984892.1	2198	15
41	BH-95	480025.9	984927.6	2198	15
42	BH-96	480052	984937.9	2200	15
43	BH-97	480252.7	984905.8	2201	15
44	BH-98	480272.2	984888.3	2201	15
45	BH-99	480270.5	984863.6	2200	15
46	BH-100	480267.5	984834.4	2199	15
47	BH-101	480261.4	984808	2199	15
48	BH-102	480237.5	984796.9	2198	15
49	BH-106	480190.6	984947	2202	10
50	BH-107	480212.6	985007.9	2202	10
51	BH-108	480212.6	984944.4	2202	10
52	BH-109	480261.3	984941.6	2202	10
53	BH-110	480281.7	984957.2	2203	10
54	BH-112	480093.4	985005.1	2202	10
55	BH-113	480122.9	984993.6	2202	10
56	BH-114	480095.2	985026.6	2203	10
57	BH-115	480127.8	985029.2	2204	10
58	BH-127	480199	985019.8	2204	10
59	BH-128	480230.8	985007.8	2204	10
60	BH-129	480194.1	984983.3	2203	10
61	BH-130	480224.9	984987	2203	10
62	BH-103	480046.3	984971	2200	15
63	BH-104	480077.5	984967.6	2201	15
64	BH-105	480103.4	984963.9	2201	15
65	BH-111	480036.9	984996.5	2201	15
66	BH-116	480043.3	985047.3	2202	15
67	BH-117	480061.6	985073.9	2203	15
68	BH-118	480091	985065.1	2204	10
69	BH-119	480118.1	985061.3	2205	10
70	BH-120	480147.2	985058.051	2205	10
71	BH-121	480174.9	985054.7	2205	10
72	BH-122	480208.1	985053.5	2205	10
73	BH-123	480228.6	985045.1	2205	10
74	BH-124	480250.3	985039.9	2205	10
75	BH-125	480272.3	985018.4	2205	10
76	BH-126	480287.3	984999	2205	10

77	BH-486	480191.8	985292.8	2205	10
78	BH-487	480191.1	985315.6	2205	10
79	BH-488	480191.8	985335.4	2205	10
80	BH-489	480168.5	985347.2	2205	10
81	BH-490	480138	985352.3	2205	10
82	BH-491	480143.3	985376.9	2204	10
83	BH-492	480171.6	985372.4	2205	10
84	BH-493	480198	985375.5	2205	10
85	BH-494	480201.6	985392.4	2205	10
86	BH-495	480210	985415.5	2205	10
87	BH-476	480118.3	985398.3	2203	15
88	BH-477	480114.1	985372.9	2203	15
89	BH-478	480110.6	985341.2	2203	15
90	BH-479	480105.6	985314.2	2204	15
91	BH-480	480104.2	985278.7	2204	15
92	BH-481	480122.9	985260.3	2205	15
93	BH-482	480144.5	985258.9	2205	15
94	BH-483	480175.6	985254.1	2205	15
95	BH-484	480212.8	985253.3	2205	15
96	BH-485	480216.4	985281.4	2206	15
97	BH-496	480163.4	985443.6	2204	15
98	BH-497	480181.4	985467.4	2205	15
99	BH-498	480209.9	985463.6	2205	15
100	BH-499	480238	985459	2207	15

Appendix B Artificial neural network analysis data silty clay soil (at depth 1.5-2.0)

Model 1: Data for Correlation of undrained shear strength (Cu) with index tests

Sr. No.	BH-ID	Depth	Pd	wet sieve analysis (AASHTO T27)			Atterberg limit (AASHTO T89&90)			USCS	Cu	LLm	Pim
				2 mm	0.425 mm	0.075 mm	LL	PL	PI				
1	BH-58	1.55-2.00	17.4	85	70.5	59	77	49	28	MH	39.76	54.28	32.13
2	BH-61	1.55-1.95	16.2	97.4	94.2	91	68	46	22	CH	33.62	64.05	46.38
3	BH-62	1.55-1.95	17.1	100	99.9	98.9	95	49	46	CH	96.78	94.90	43.48
4	BH-75	1.55-2.00	16.7	99.4	98.2	96.9	68	48	20	CH	36.3	66.77	38.35
5	BH-78	1.55-2.00	16.6	99.9	99.6	99.1	95	51	44	CH	31.4	94.62	42.19
6	BH-79	1.50-1.60	17	99.9	99.7	99.2	76	43	33	CH	35.7	75.77	40.94
7	BH-80	1.55-2.00	17.1	99.9	99.7	99.1	98	55	43	CH	51.6	97.70	33.75
8	BH-81	1.55-2.00	16.4	99.9	99.5	98.9	93	53	40	CH	42.35	92.53	43.7
9	BH-82	1.55-2.00	16.5	99.6	99.4	98.8	89	52	37	CH	34.95	88.46	43.66
10	BH-84	1.55-2.00	17	99.8	99	97.9	94	50	44	CH	34.65	93.06	47.99
11	BH-85	1.55-2.00	16.7	99.9	99.4	97.8	95	50	45	CH	34.11	94.43	41.47
12	BH-91	1.55-2.00	16.9	98	97.7	97.3	107	58	49	CH	35.1	104.5	42.96
13	BH-92	1.50-1.95	16.9	99.8	99.5	99.3	96	55	41	CH	61.3	95.52	50.66
14	BH-93	1.50-1.95	16.2	91.5	90.7	90.1	100	51	49	CH	63.15	90.7	44.67
15	BH-94	1.50-1.95	16.9	99.6	99.4	98.3	98	55	43	CH	33.35	97.41	54.35
16	BH-95	1.50-1.95	15.4	99.5	98.8	98.2	93	49	44	CH	27.4	91.88	51.49
17	BH-96	1.50-1.95	17.1	99.9	99.7	99.5	99	52	47	CH	30.05	98.70	37.08
18	BH-86	1.50-1.95	17.4	99.9	99.4	98.9	97	51	46	CH	35.65	96.41	48.88
19	BH-87	1.50-1.95	17	95.6	94.8	81	98	53	45	CH	44.55	92.90	43.67
20	BH-88	1.50-1.95	17.4	99.1	96.5	91.7	98	55	43	CH	43.6	94.57	45.43
21	BH-98	1.50-1.95	17.7	99.8	99.2	98.7	94	51	43	CH	37.6	93.24	43.81
22	BH-99	1.50-1.95	17	100	99.9	99.6	100	51	49	CH	33.8	99.9	53.03
23	BH-100	1.50-1.95	17.1	99.9	99.5	98.9	93	52	41	CH	35.6	92.53	47.27
24	BH-101	1.50-1.95	17	97.2	97	96.2	90	47	43	CH	27.8	87.3	53.89
25	BH-102	1.50-1.95	16.9	99.9	99.7	99.4	99	56	43	CH	30	98.70	50.28
26	BH-106	1.55-2.00	16.7	99.9	99.5	98.6	LL	PL	PI	CH	cu	94.52	51.88
27	BH-107	1.55-2.00	17.4	99.9	99.6	99.1	95	51	44	CH	33.6	103.5	33.75
28	BH-108	1.55-2.00	16.7	100	99.8	99.3	104	54	50	CH	40.9	97.80	11.86
29	BH-109	1.55-2.00	16.9	99.8	99.7	99	98	50	48	CH	39.15	77.76	42.11
30	BH-112	1.50-1.95	16.5	99.9	99.4	98.8	78	46	32	CH	28.4	103.3	41.55

31	BH-113	1.50-1.95	18.9	99.6	99	97.2	104	54	50	CH	34.55	98.01	30.84
32	BH-114	1.50-1.95	16.9	99.6	99	98.1	99	52	47	CH	35.23	93.06	27.07
33	BH-115	1.50-1.95	16.4	92	90.7	90	94	50	44	CH	36.45	67.11	47.26
34	BH-127	1.50-1.95	16.9	100	99.8	99.4	74	39	35	CH	53.3	98.80	39.72
35	BH-128	1.50-1.95	17.3	99.5	98.8	97.4	99	54	45	CH	55.95	76.07	50.54
36	BH-129	1.50-1.95	17.3	99.8	99.4	99	77	43	34	CH	48.01	53.67	47.32
37	BH-130	1.55-2.00	16.1	99.8	99.4	99	54	54	50	CH	45.55	48.70	39.48
38	BH-487	1.55-2.00	17	99.7	99.6	99	49	49	39	CH	60.4	107.5	33.63
39	BH-489	1.55-2.00	16.5	63.4	59.5	56	108	58	50	CH	36.15	33.32	23.46
40	BH-493	1.55-2.00	17.3	100	99.8	93	56	35	21	CH	38.55	92.81	29.01
41	BH-494	1.55-2.00	16.9	99.9	99.7	99.4	93	52	41	CH	22.7	95.71	42.08
42	BH-476	1.55-2.00	16.7	99.6	99.5	99.3	96	52	44	CH	24.9	86.55	39.69
43	BH-481	1.55-2.00	17.3	99.4	98.6	97.4	87	47	40	CH	38.8	92.68	34.36
44	BH-483	1.55-2.00	16.5	95.1	93.8	92.4	94	50	44	CH	38.9	94.73	36.03
45	BH-497	1.55-2.00	17	99.9	99.7	99.3	101	53	48	CH	37.9	98.70	30.5
46	BH-498	1.55-2.00	16.7	100	99.9	99.3	99	52	47	CH	38.2	99.9	24.26

Appendix C Artificial neural network silty clay soil (at depth 3.0m-5.45m)

Model 2: Data for Correlation of undrained shear strength (Cu) with index tests

			wet sieve analysis (AASHTO T27)			Atterberg limit (AASHTO T89&90						
Sr.No.	BH-ID	Depth	2mm	0.425mm	0.075mm	LL	PL	PI	USCS	Cu	LLm	Pim
1	BH-53	1.55-2.00	77.1	69.3	50.8	46	35	11	SM	26.58	31.878	24.3
2	BH-54	1.55-2.00	90.49	83.6	74.1	64	48	16	MH	38.64	53.504	40.1
3	BH-55	1.55-2.00	87	78.2	67.5	66	44	22	MH	29.22	51.612	34.4
4	BH-55	4.55-5.00	51.2	41.5	32.1	49	33	16	SM	30.9	20.335	13.7
5	BH-56	1.55-2.00	55	42.1	39.5	37	24	13	SM	40.24	15.577	10.1
6	BH-56	4.55-5.00	70.5	61.1	46.4	60	44	16	SM	33.73	36.66	26.9
7	BH-57	1.55-2.00	75.2	64.9	58.7	55	31	24	MH	18.68	35.695	20.1
8	BH-57	4.55-5.00	68.7	59.8	49.9	56	37	19	SM	30.98	33.488	22.1
9	BH-58	4.55-5.00	45.9	32	25.1	33	27	6	SM	39.76	10.56	8.64
10	BH-59	1.55-2.00	93	88.7	82.8	56	40	16	MH	31.5	49.672	35.5
11	BH-60	4.55-5.00	78.8	71.6	59.2	54	36	18	SM	40.5	38.664	25.8
12	BH-61	4.50-4.95	80.1	62.7	47.1	49	33	16	SM	33.62	30.723	20.7
13	BH-62	3.10-3.55	91.8	88.6	86.9	67	40	27	MH	96.78	59.362	35.4
14	BH-62	4.50-4.95	54.4	49.9	42.6	42	29	13	SM	40.44	20.958	14.5
15	BH-63	1.55-1.60	61.5	45.7	33.6	46	37	9	SM	33.63	21.022	16.9
16	BH-64	1.55-2.00	70.8	55.3	41.5	44	33	11	SM	19.14	24.332	18.2
17	BH-66	1.50-1.55	70.6	59.7	57.3	30	23	7	ML	26.37	17.91	13.7
18	BH-70	1.50-1.95	53.5	50.9	46.1	59	37	22	SM	35.04	30.031	18.8
19	BH-71	1.55-1.60	73.4	64.7	49.3	43	28	15	SM	34.62	27.821	18.1
20	BH-72	1.55-1.60	85.8	81.1	79	50	33	17	MH	28.86	40.55	26.8
21	BH-73	1.55.1.95	96.3	87.9	79.4	60	42	18	MH	24.37	52.74	36.9
22	BH-73	4.55-5.00	80.7	64.7	50.3	43	32	11	SM	35.5	27.821	20.7
23	BH-74	3.00-3.55	78	65.8	63.9	45	36	9	ML	33.4	29.61	23.7
24	BH-74	4.50-4.95	65.5	47	43.6	40	29	11	SM	31.34	18.8	13.6
25	BH-78	3.10-3.55	99.9	99.7	99	98	53	45	CH	31.4	97.706	52.8
26	BH-78	4.50-4.95	99.9	99.7	99.3	99	55	44	CH	46	98.703	54.8
27	BH-97	3.10-3.55	99.5	99.2	98.1	88	45	43	CH	39.45	87.296	44.6

Appendix D Artificial neural network clayey silty sand (at depth 1.5m-5.0m)

Model 3: Data for Correlation of undrained shear strength (Cu) with index tests

				wet sieve analysis (AASHTO T27)			Atterberg limit (AASHTO T89&90						
Sr. No.	BH-ID	depth	ρd	2 mm	0.425 mm	0.075 mm	LL	PL	PI	USCS	Cu	PIm	LLm
1	BH-58	3.00-3.45	16.7	77.1	66.6	56	46	31	15	SM	39.76	30.63	9.99
2	BH-60	3.10-3.45	17.4	86.6	83.6	79.5	42	25	17	ML	40.5	35.11	14.21
3	BH-61	3.10-3.55	16.7	91.9	72.1	59.4	61	43	18	SM	33.62	43.98	12.97
4	BH-75	3.10-3.55	16.8	99.9	99.6	99.2	96	51	45	CH	36.3	95.61	44.82
5	BH-79	3.10-3.55	16.4	99.9	99.6	99.1	98	53	45	CH	35.7	97.60	44.82
6	BH-80	3.10-3.55	18.8	99.9	99.5	98.8	99	52	47	CH	51.6	98.50	46.76
7	BH-81	3.10-3.55	16.8	99.8	99.6	99.4	87	47	40	CH	42.35	86.62	39.84
8	BH-82	3.10-3.55	16.3	99.8	99.7	98.9	71	38	33	CH	34.95	70.78	32.90
9	BH-84	3.10-3.55	15.9	99.5	98.6	97.5	87	48	39	CH	34.65	85.78	38.45
10	BH-85	3.10-3.55	17.1	99.9	99.5	98.8	86	46	40	CH	34.11	85.57	39.8
11	BH-90	3.10-3.55	16.9	99.9	99.5	98	94	51	43	CH	60.6	93.53	42.78
12	BH-91	3.10-3.55	15.8	99.3	99	98.7	92	50	42	CH	35.1	91.08	41.58
13	BH-92	3.10-3.55	15.9	100	99.6	99.3	94	57	37	CH	61.3	93.62	36.85
14	BH-93	3.10-3.55	16.9	92.1	91.6	91.1	97	53	44	CH	63.15	88.85	40.30
15	BH-94	3.00-3.45	16.8	99.9	99.8	99.4	96	54	42	CH	33.35	95.80	41.9
16	BH-95	3.00-3.45	16.6	99.7	99.1	98.4	97	54	43	CH	27.4	96.12	42.61
17	BH-96	3.00-3.45	15.9	98.9	98.7	97.9	93	93	44	CH	30.05	91.79	43.42
18	BH-86	3.10-3.55	17.1	99.8	99.3	98.7	89	48	41	CH	35.65	88.37	40.71
19	BH-87	3.10-3.55	16.9	99.4	99.2	98	81	52	29	CH	44.55	80.35	28.76
20	BH-88	3.10-3.55	16.8	99.6	99.1	98.6	90	53	37	CH	43.6	89.19	36.66
21	BH-98	3.00-3.45	17.2	99.9	99.6	99.2	92	50	42	CH	37.6	91.63	41.83
22	BH-99	3.00-3.45	16.1	99.9	99.5	99	80	44	36	CH	33.8	79.6	35.82
23	BH-100	3.00-3.45	17.1	99.9	99.6	99.1	92	49	43	CH	35.6	91.63	42.82
24	BH-101	3.00-3.45	16.8	99.96	99.8	99	88	54	34	CH	27.8	87.82	33.93
25	BH-102	3.00-3.45	17.9	99.8	99.5	99	94	53	41	CH	30	93.53	40.79
26	BH-106	3.00-3.45	17.1	99.6	99.3	98.9	98	55	43	CH	33.6	97.31	42.69
27	BH-107	3.00-3.45	17.2	99.8	99.2	98.4	95	50	45	CH	40.9	94.24	44.64
28	BH-108	3.00-3.45	17.2	99.9	99.5	98.9	96	55	41	CH	39.15	95.52	40.79
29	BH-109	3.00-3.45	17.2	100	99.8	99.3	88	46	42	CH	28.4	87.82	41.91
30	BH-110	3.00-3.45	16.1	99.7	99.4	98.9	96	51	45	CH	36.75	95.42	44.73
31	BH-112	3.10-3.55	16.9	99.8	99.2	98.5	97	54	43	CH	34.55	96.22	42.65
32	BH-113	3.10-3.55	16.4	99.9	99.8	99.5	84	45	39	CH	35.23	83.83	38.92
33	BH-114	3.10-3.55	17.2	99.9	99.2	98.3	87	47	40	CH	36.45	86.30	39.68

34	BH-115	3.10-3.55	16.8	84	80.3	79.3	86	56	30	CH	53.3	69.05	24.09
35	BH-127	3.10-3.55	16.7	100	99.8	99.5	98	53	45	CH	55.95	97.80	44.91
36	BH-128	3.10-3.55	16.2	99.8	99.3	98.7	104	67	47	CH	48.01	103.2	46.67
37	BH-129	3.10-3.55	16.8	90.5	88.7	87.7	45	45	42	CH	45.55	39.91	37.25
38	BH-130	3.00-3.45	16.3	99.8	99.4	99	51	51	43	CH	60.4	50.69	42.74
39	BH-486	3.00-3.45	16.9	98.2	97.3	96.9	92	51	41	CH	37.5	89.51	39.89
40	BH-487	3.00-3.45	16.8	99.9	99.7	99.3	95	50	45	CH	36.15	94.71	44.86
41	BH-488	3.00-3.45	16.6	100	99.8	99.3	93	52	41	CH	48.18	92.81	40.91
42	BH-489	3.00-3.45	16.8	100	99.8	92	92	51	41	CH	38.55	91.81	40.91
43	BH-490	3.00-3.45	16.3	99.9	99.9	98	98	50	48	CH	42.55	97.90	47.95
44	BH-491	3.00-3.45	15.9	99.9	99.5	81	81	49	32	CH	38.62	80.59	31.84
45	BH-492	3.00-3.45	17.1	99.7	99.5	92	92	49	43	CH	33.1	91.54	42.78
46	BH-493	3.00-3.45	16.9	100	99.8	93	93	51	42	CH	22.7	92.81	41.91
47	BH-495	3.00-3.45	17.2	100	99.6	98.6	91	53	38	CH	24.9	90.63	37.84
48	BH-476	3.00-3.45	16.8	99.6	99.4	99.1	92	48	44	CH	38.8	91.44	43.73
49	BH-477	3.00-3.45	16.7	99.7	99.5	99	91	48	43	ML	34.4	90.54	42.78
50	BH-478	3.00-3.45	16.2	99.8	98.9	98.2	98	52	46	CH	37.3	96.92	45.49
51	BH-479	3.00-3.45	16.8	99.6	99.1	98.7	91	49	42	CH	43.05	90.18	41.62
52	BH-480	3.00-3.45	16.3	99.7	98.9	97.2	97	50	47	CH	42.1	95.93	46.48
53	BH-481	3.00-3.55	16.9	99.5	98.8	97.3	84	44	40	CH	38.9	82.99	39.52
54	BH-482	3.00-3.55	17.4	99.6	98.7	98	89	48	41	CH	37.4	87.84	40.46
55	BH-483	3.00-3.55	16.7	99.5	98.3	97.2	93	50	43	CH	37.9	91.42	42.27
56	BH-484	3.00-3.55	16.8	99.6	98.6	97.7	93	53	40	CH	36.55	91.69	39.44
57	BH-485	3.00-3.55	16.4	99.6	98.7	97.8	93	50	43	CH	30.1	91.79	42.44
58	BH-496	3.00-3.55	16.8	100	99.9	99.6	88	51	37	CH	42	87.91	36.96
59	BH-497	3.00-3.55	16.3	100	99.9	99.6	96	50	46	CH	38.2	95.90	45.95
60	BH-498	3.00-3.55	17.2	100	99.8	99.5	96	52	44	CH	42.55	95.80	43.91
61	BH-499	3.00-3.55	16.8	99.9	99.7	99.3	90	47	43	CH	37.5	89.73	42.87

Appendix E Artificial neural network data of fine grained soil (at depth 2.50-3.10m)

Model 1: Data for Correlation of swelling pressure (Ps) with index tests

Sr. No.	BH-ID	Depth(m)	ρd,	NMC	LL	PI	PL	Ps Kpa
1	BH-97	2.50-3.10	12.41	42.61	88	45	43	35.6
2	BH-79	2.50-3.10	12.68	46.54	98	53	45	30.1
3	BH-85	2.50-3.10	11.23	48.9	86	46	40	25.5
4	BH-106	2.50-3.10	12.46	48.25	87	48	39	34.3
5	BH-115	2.50-3.10	11.72	46.46	88	47	44	41
6	BH-127	2.50-3.10	12.35	40.86	86	47	39	42.3
7	BH-478	2.50-3.10	11.3	35.35	98	52	46	30.2
8	BH-482	2.50-3.10	12.8	24.86	98	48	41	43.7
9	BH-488	2.50-3.10	12.56	36.44	93	52	41	49.6
10	BH-491	2.50-3.10	11.71	32.57	79	46	33	35.7
11	BH-497	2.50-3.10	11.24	30.61	93	52	41	28.6
12	BH-75	2.50-3.10	11.78	35.47	96	51	45	37.3
13	BH-78	2.50-3.10	10.44	49.49	98	53	45	32.1
14	BH-82	2.50-3.10	12.79	43.01	71	38	33	35.5
15	BH-84	2.50-3.10	11.58	42.25	88	49	39	36.3
16	BH-90	2.50-3.10	11.1	48.32	76	47	29	42.7
17	BH-98	2.50-3.10	13.08	42.61	81	43	38	39.8
18	BH-100	2.50-3.10	11.42	49.93	92	49	43	39.4
19	BH-102	2.50-3.10	10.86	55.19	87	48	37	45.8
20	BH-107	2.50-3.10	12.45	38.85	97	52	47	37.4
21	BH-112	2.50-3.10	12.22	36.63	95	52	41	41.3
22	BH-129	2.50-3.10	12.49	35.63	95	54	40	45.3

Appendix F Conventional regression analysis for model 1

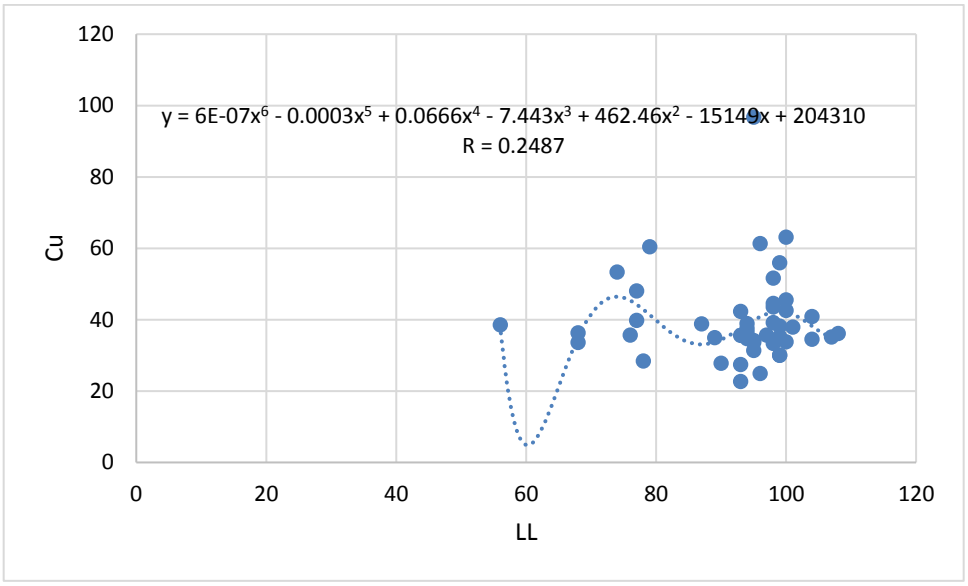

Figure F-1 Regression analysis (model-1) between Cu and LL

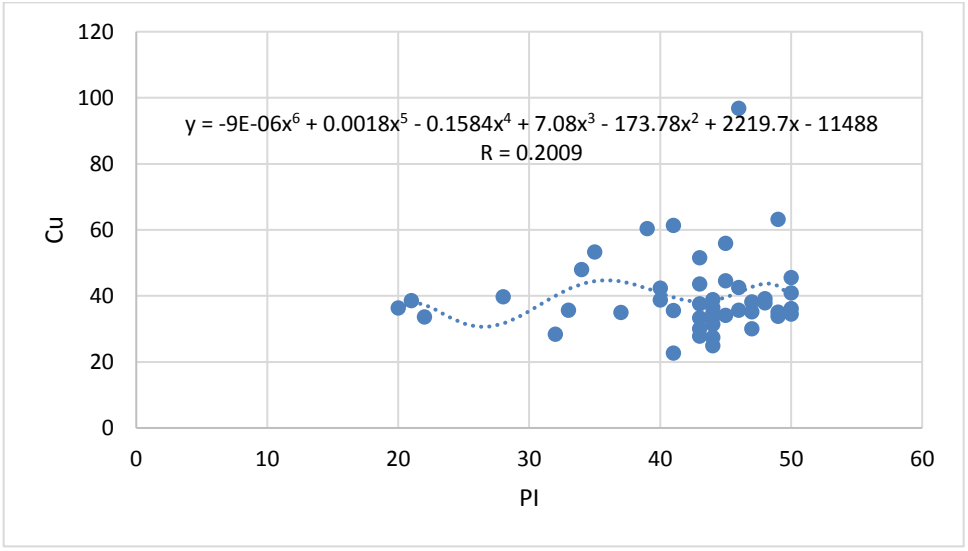

Figure F-2 Regression analysis (model-1) between Cu and PI

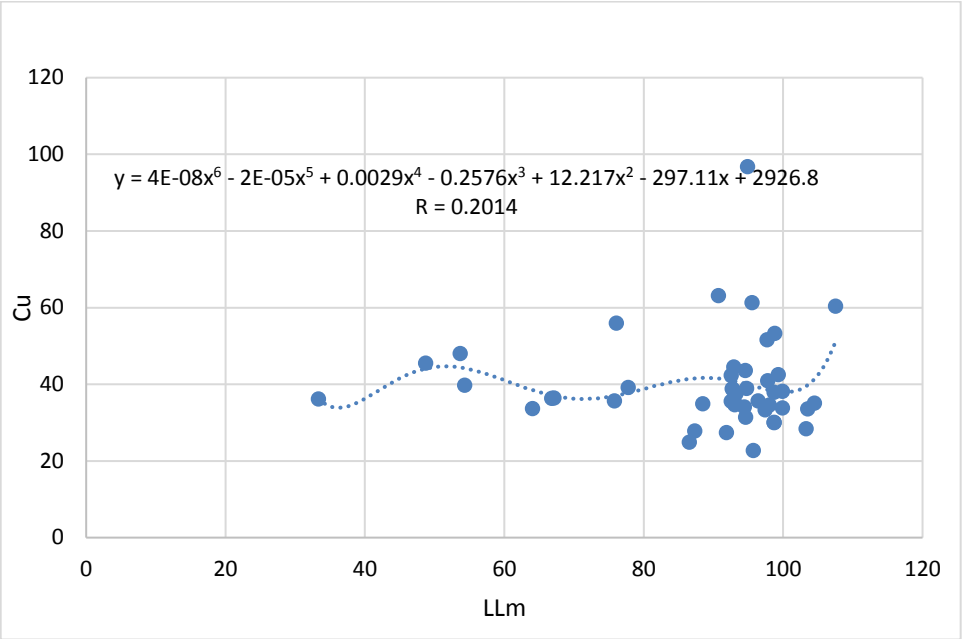

Figure F-3 Regression analysis (model-1) between Cu and LLm

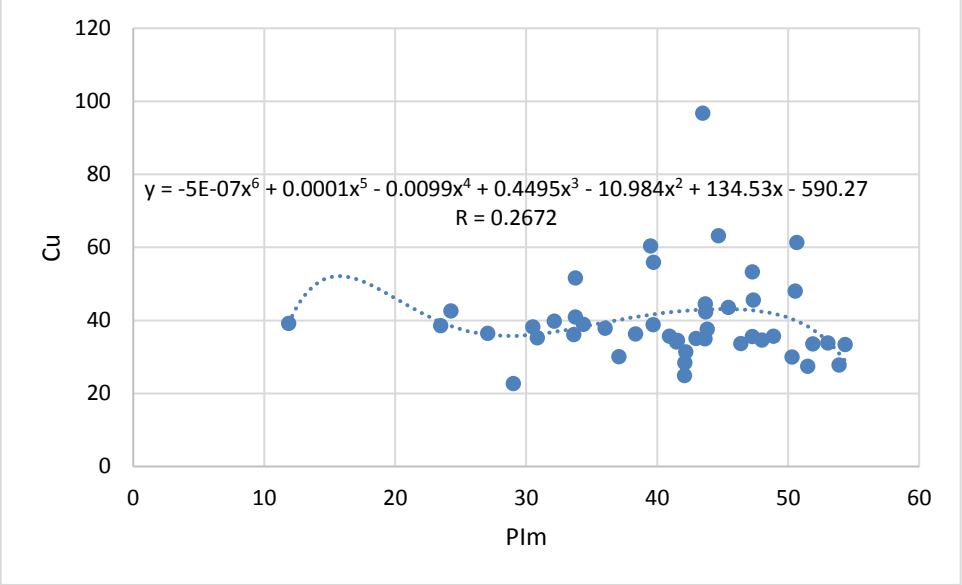

Figure F-4 Regression analysis (model-1) between Cu and PIm

Appendix G Conventional regression analysis for model 2

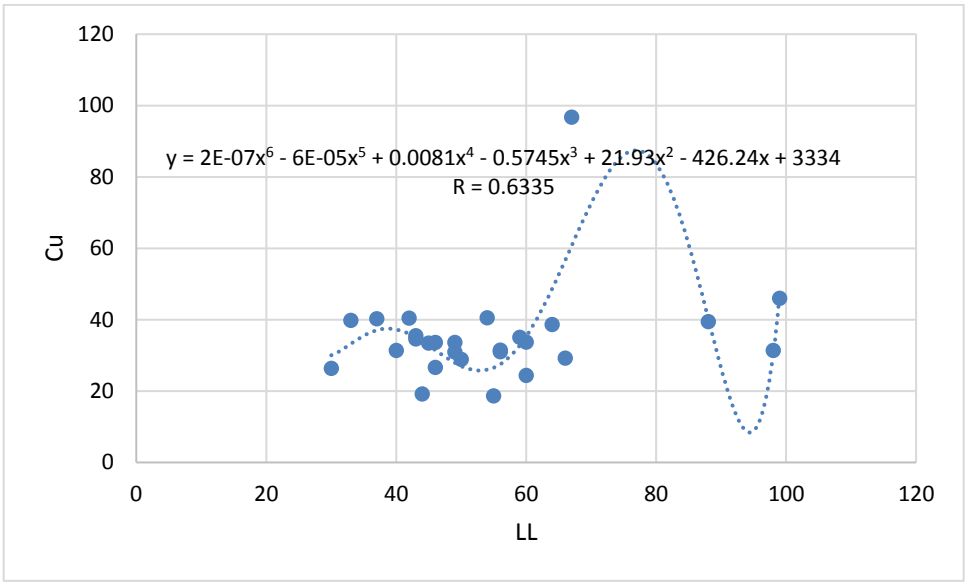

Figure G-1 Regression analysis (model-2) between Cu and LL

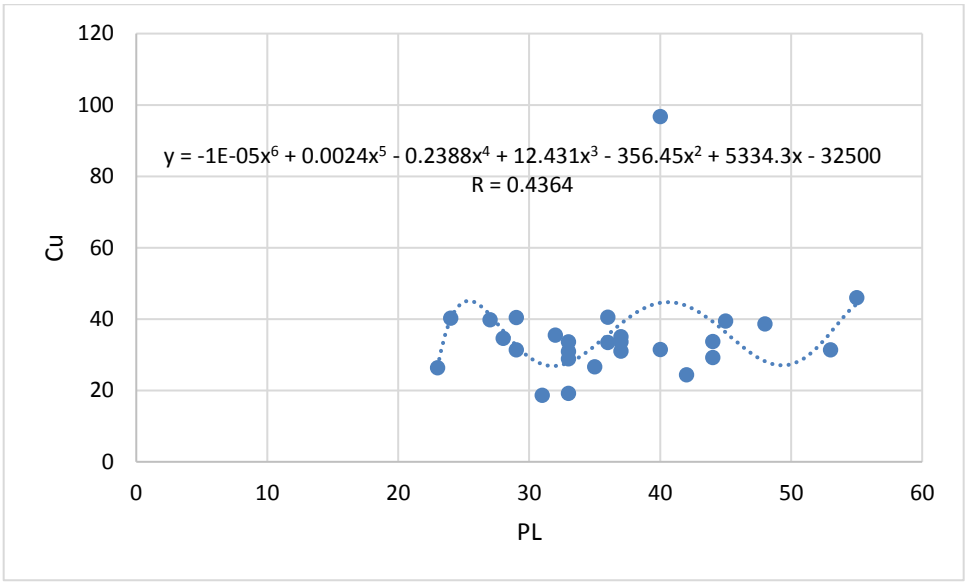

Figure G-2 Regression analysis (model-2) between Cu and PL

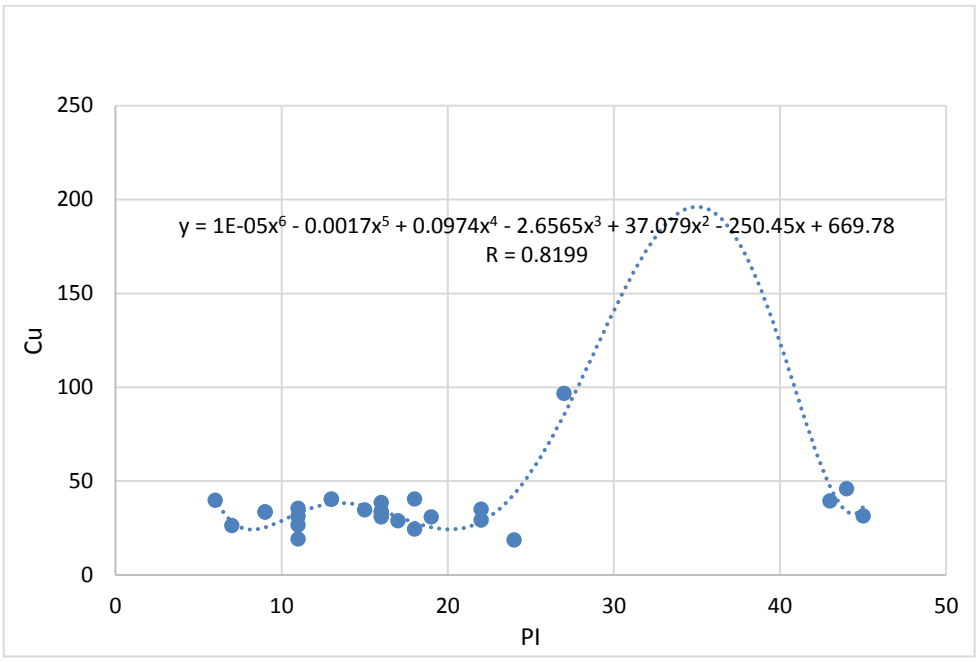

Figure G-3 Regression analysis (model-2) between Cu and PI

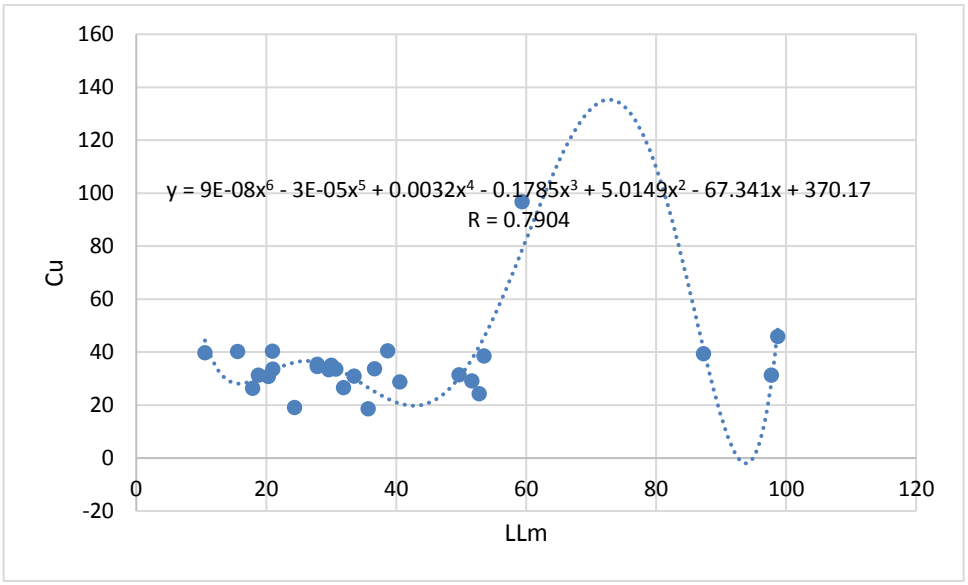

Figure G-4 Regression analysis (model-2) between Cu and LLm

Appendix H Conventional regression analysis for model 3

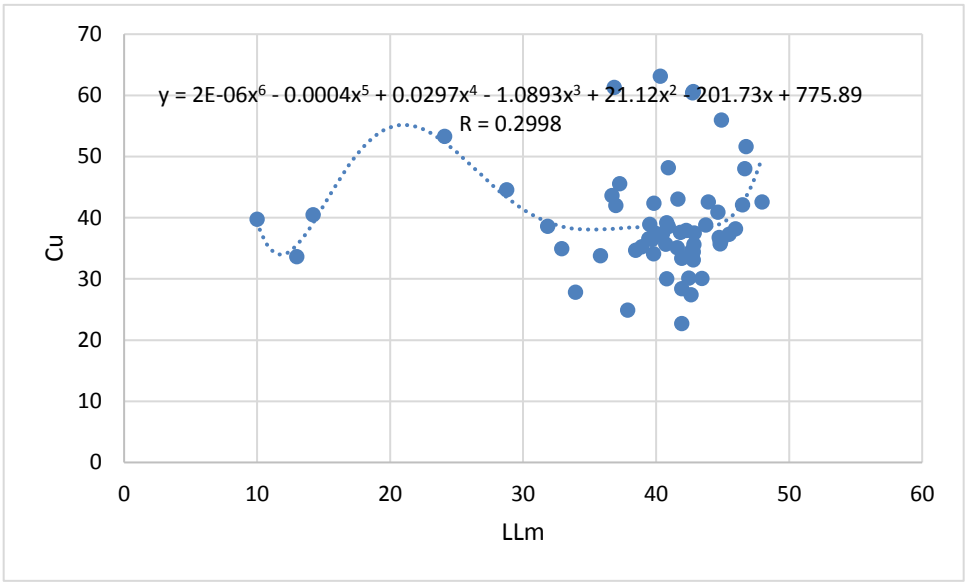

Figure H-1 Regression analysis (model-3) between Cu and LLm

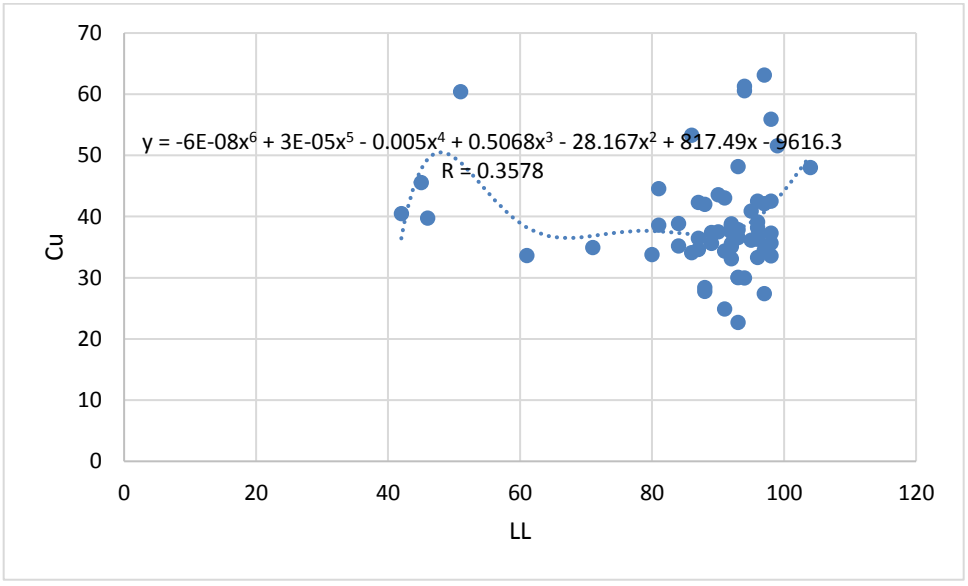

Figure H-2 Regression analysis (model-3) between Cu and LL

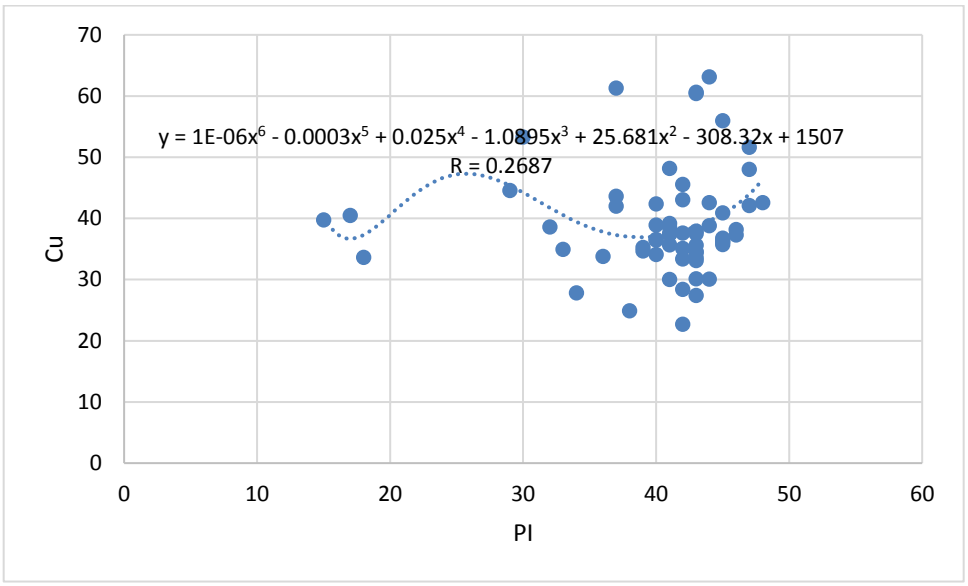

Figure H-3 Regression analysis (model-3) between Cu and PI

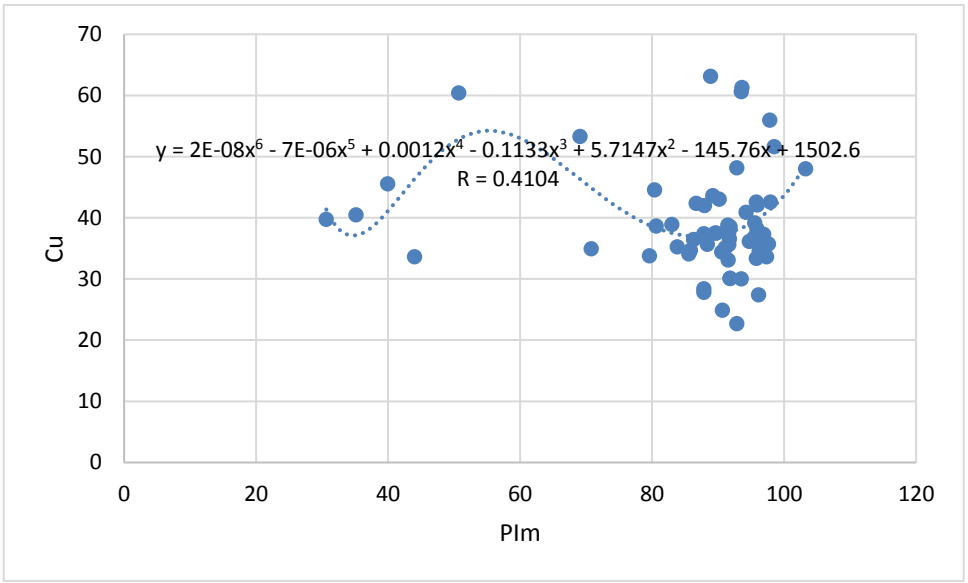

Figure H-4 Regression analysis (model-3) between Cu and PIm

Appendix I Conventional regression analysis for swelling pressure

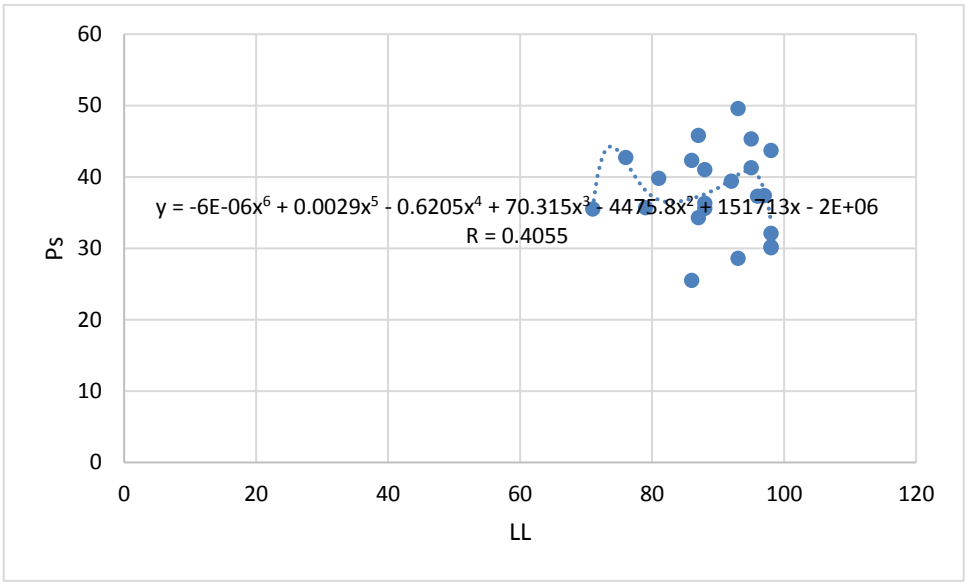

Figure I-1 Regression analysis (model-1) between Ps and LL

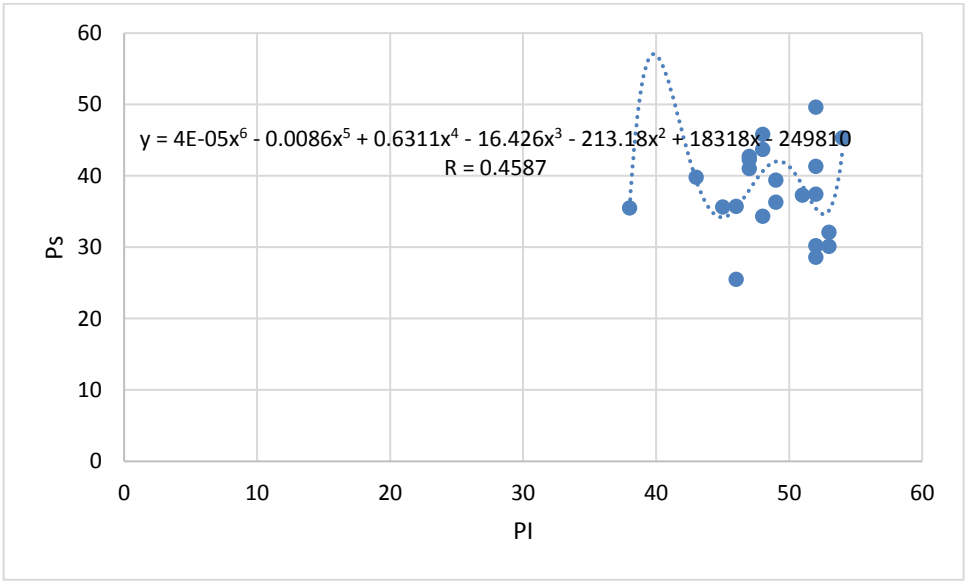

Figure I-2 Regression analysis (model-1) between Ps and PI

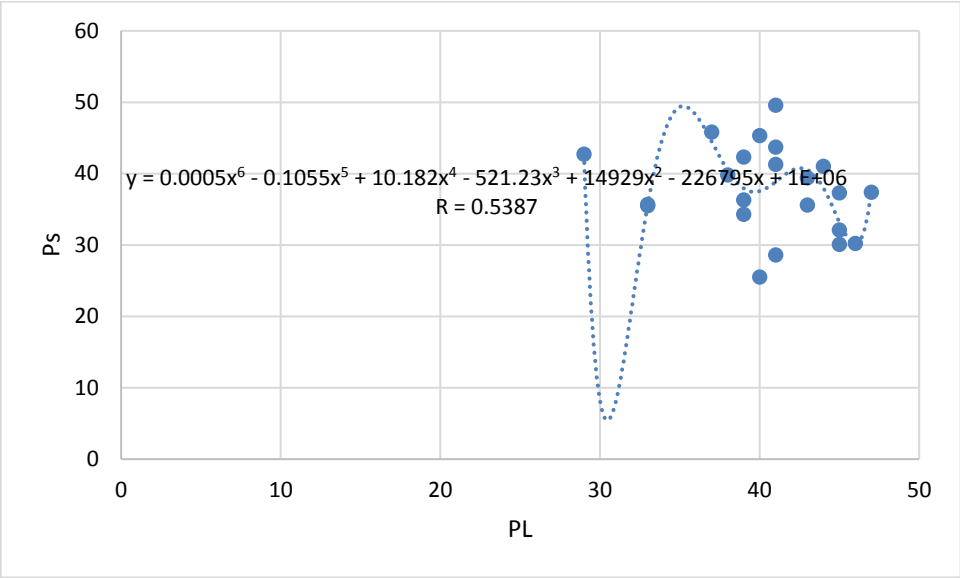

Figure I-3 Regression analysis (model-1) between Ps and PL

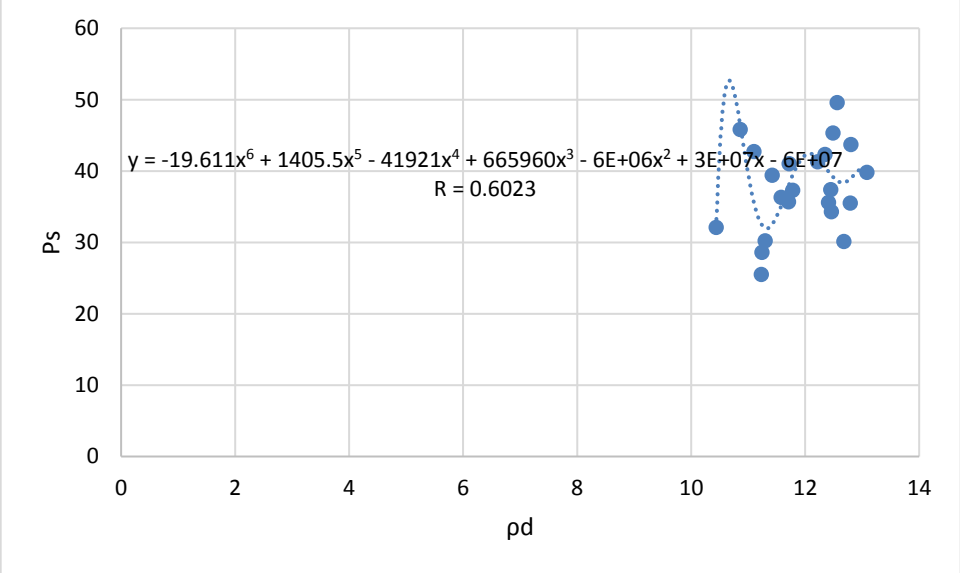

Figure I-4 Regression analysis (model-1) between Ps and ρ_d

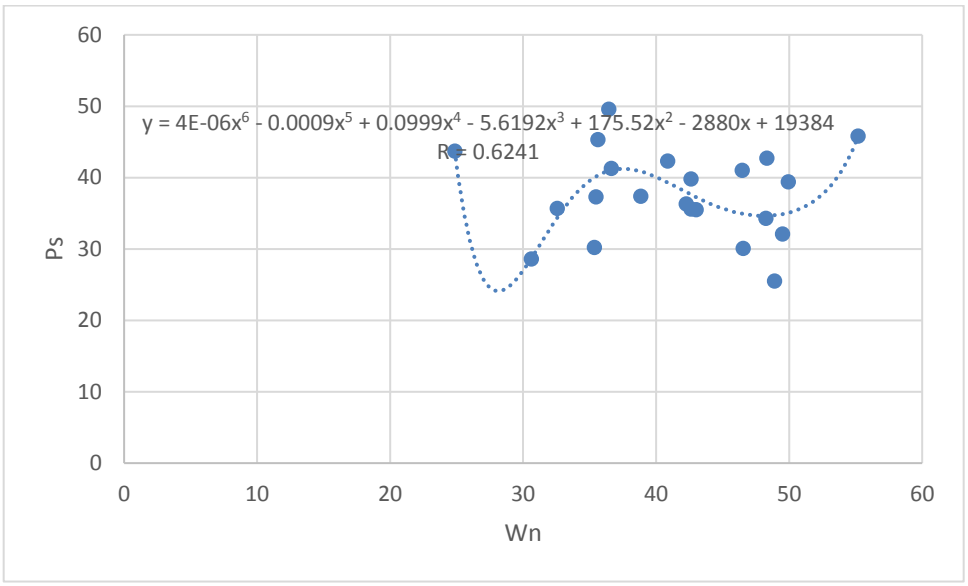

Figure I-5 Regression analysis (model-1) between Ps and Wn

Appendix J Artificial neural network matlab script for optimization of model 1 (LL Vs Cu)

```
clc
clear all
close all
data = xlsread('model1.xlsx', 'sheet1');
x = data(:, 1);
t = data(:, 2);
n = length(t);
% data transformation
t2 = log(1+t); %t2 = t; % t2 = 1/t; % t2 = sqrt(t); % t2 = t.^2;
%
x2 = zeros(46,1); %prelocating memory
minx = min(x);
maxx = max(x);
for i = 1:size(x,1)
    for j = 1:size(x,2)
        x2(i,j) = (x(i,j)-minx(j))/(maxx(j)-minx(j));
    end
end
xt = x2';
tt = t2';
%
rmse_train= zeros(60,1);
rmse_test = zeros(60,1);
rmse_val = zeros(60,1);
r_train= zeros(60,1);
r_test = zeros(60,1);
r_val = zeros(60,1);
r_all = zeros(60,1);

for i = 1:60
    %architecture of the ANN
    hiddenLayerSize = i;
    net = feedforwardnet(hiddenLayerSize, 'trainlm');
    net.layers{1}.transferFcn = 'logsig';
%   net.layers{1}.transferFcn = 'logsig';
%   net.layers{2}.transferFcn = 'purelin';
    net.divideParam.trainRatio = 70/100;
    net.divideParam.valRatio = 15/100;
    net.divideParam.testRatio = 15/100;
    rand('seed', 1);
%   disp(rand);
    net.layers{1}.initFcn = 'initwb';
    net.inputweights{1,1}.initFcn = 'rands';
    net.layerweights{2,1}.initFcn = 'rands';
    net.biases{1,1}.initFcn = 'rands';
    net.biases{2,1}.initFcn = 'rands';
```

```
    net = init(net);
    net.trainParam.epochs = 1200;
    net.trainParam.goal = 0.01;

    %training the ANN
    [net,tr]= train(net, xt, tt);
    w1 = net.Iw{1,1};
    b1 = net.b{1};
    w2 = net.Lw{2,1};
    b2 = net.b{2};
  % w3 = net.Lw{3,2};
  % b3 = net.b{3};

    %determining the error & Performance of the ANN network
    trainoutput = exp(net(xt(:,tr.trainInd)))-1;
    traintarget = exp(tt(tr.trainInd))-1;
    e1 = traintarget-trainoutput;
    rmse_train(i) = sqrt(mean((e1).^2));
%
    valoutput = exp(net(xt(:,tr.valInd)))-1;
    valtarget = exp(tt(tr.valInd))-1;
    e2 = valtarget-valoutput;
    rmse_val(i) = sqrt(mean((e2).^2));
%
    testoutput = exp(net(xt(:,tr.testInd)))-1;
    testtarget = exp(tt(tr.testInd))-1;
    e3 = testtarget-testoutput;
    rmse_test(i) = sqrt(mean((e3).^2));
%
output = [trainoutput'; valoutput'; testoutput'];
target = [traintarget'; valtarget'; testtarget'];

r_train(i)= sum((trainoutput-mean(trainoutput)).*(traintarget-
mean(traintarget)))/sqrt(sum((trainoutput-
mean(trainoutput)).^2)*sum((traintarget-mean(traintarget)).^2));

r_val(i)= sum((valoutput-mean(valoutput)).*(valtarget-
mean(valtarget)))/sqrt(sum((valoutput-
mean(valoutput)).^2)*sum((valtarget-mean(valtarget)).^2));

r_test(i)= sum((testoutput-mean(testoutput)).*(testtarget-
mean(testtarget)))/sqrt(sum((testoutput-
mean(testoutput)).^2)*sum((testtarget-mean(testtarget)).^2));

r_all(i)= sum((output-mean(output)).*(target-
mean(target)))/sqrt(sum((output-mean(output)).^2)*sum((target-
mean(target)).^2));
end

r = [r_all r_train r_val r_test];
rmse_all = [rmse_all rmse_train rmse_val rmse_test];
```

Appendix K Proposed artificial neural network matlab script for model 1 (LL Vs Cu)

```
clc
clear all
close all
% Import
data = xlsread('model1.xlsx', 'sheet1');
x = data(:, 1);
t = data(:, 2);
n = length(t);
% normalization and transformation
t2 = log(1+t); % t2 = t^2 % t2 = rad(t) % t2 = exp(t) % t2 = 1/t
x2 = zeros(46,1); %prelocating memory
minx = min(x);
maxx = max(x);
for i = 1:size(x,1)
    for j = 1:size(x,2)
        x2(i,j) = (x(i,j)-minx(j))/(maxx(j)-minx(j));
    end
end
t1 = cputime;
% data division and training the ANN
xt = x2';
tt = t2';
hiddenLayerSize = 8; %use[] to add hidden layers
net = feedforwardnet(hiddenLayerSize, 'trainlm');
net.layers{1}.transferFcn = 'logsig';
% net.layers{2}.transferFcn = 'logsig';
% net.layers{3}.transferFcn = 'purelin';
net.divideParam.trainRatio = 70/100;
net.divideParam.valRatio = 15/100;
net.divideParam.testRatio = 15/100;
rand('seed', 1);
% disp(rand);
net.layers{1}.initFcn = 'initwb';
net.inputweights{1,1}.initFcn = 'rands';
net.layerweights{2,1}.initFcn = 'rands';
net.biases{1,1}.initFcn = 'rands';
net.biases{2,1}.initFcn = 'rands';
net = init(net);
net.trainParam.epochs = 1200;
net.trainParam.goal = 0.01;
[net,tr]= train(net, xt, tt);
% weight, bias & Performance of the ANN network
TrTime = cputime - t1;
w1 = net.Iw{1,1};
b1 = net.b{1};
w2 = net.Lw{2,1};
```

```
b2 = net.b{2};
% w3 = net.Lw{3,2};
% b3 = net.b{3};
t2 = cputime;
trainoutput = exp(net(xt(:,tr.trainInd)))-1;
traintarget = exp(tt(tr.trainInd))-1;
e1 = traintarget-trainoutput;
rmse_train = sqrt(mean((e1).^2));
%
valoutput = exp(net(xt(:,tr.valInd)))-1;
valtarget = exp(tt(tr.valInd))-1;
e2 = valtarget-valoutput;
rmse_val = sqrt(mean((e2).^2));
%
testoutput = exp(net(xt(:,tr.testInd)))-1;
testtarget = exp(tt(tr.testInd))-1;
e3 = testtarget-testoutput;
rmse_test = sqrt(mean((e3).^2));
%
output = [trainoutput'; valoutput'; testoutput'];
target = [traintarget'; valtarget'; testtarget'];

r_train = sum((trainoutput-mean(trainoutput)).*(traintarget-
mean(traintarget)))/sqrt(sum((trainoutput-
mean(trainoutput)).^2)*sum((traintarget-mean(traintarget)).^2));

r_val = sum((valoutput-mean(valoutput)).*(valtarget-
mean(valtarget)))/sqrt(sum((valoutput-
mean(valoutput)).^2)*sum((valtarget-mean(valtarget)).^2));

r_test = sum((testoutput-mean(testoutput)).*(testtarget-
mean(testtarget)))/sqrt(sum((testoutput-
mean(testoutput)).^2)*sum((testtarget-mean(testtarget)).^2));

r_all = sum((output-mean(output)).*(target-
mean(target)))/sqrt(sum((output-mean(output)).^2)*sum((target-
mean(target)).^2));
% model prediction
prompt = 'what is the input value (1 by 1 matrix)? ';
xs = input(prompt);
xn = [x; xs];
minxn = min(xn);
maxxn = max(xn);
for i = 1:size(xs,1)
    for j = 1:size(xs,2)
        xs11(i,j) = (xs(i,j)-minxn(j))/(maxxn(j)-minxn(j));
    end
end
ys = sim(net, xs11');
ys2 = exp(ys(:,1))-1;
```